ANL-76-35



# HIGH-PERFORMANCE BATTERIES FOR OFF-PEAK ENERGY STORAGE AND ELECTRIC-VEHICLE PROPULSION

## Progress Report for the Period January—March 1976



U of C-AUA-USERDA

ARGONNE NATIONAL LABORATORY, ARGONNE, ILLINOIS

Prepared for the U. S. ENERGY RESEARCH AND DEVELOPMENT ADMINISTRATION under Contract W-31-109-Eng-38

Printed in the United States of America
Available from
National Technical Information Service
U. S. Department of Commerce
5285 Port Royal Road
Springfield, Virginia 22161
Price: Printed Copy $4.50; Microfiche $2.25

Distribution Category:
Energy Storage—Electrochemical
(UC-94c)

ANL-76-35

ARGONNE NATIONAL LABORATORY
9700 South Cass Avenue
Argonne, Illinois 60439

# HIGH-PERFORMANCE BATTERIES FOR OFF-PEAK ENERGY STORAGE AND ELECTRIC-VEHICLE PROPULSION

Progress Report for the Period
January—March 1976

| | |
|---|---|
| P. A. Nelson | Manager, Battery Program |
| R. O. Ivins | Associate Manager, Battery Program |
| N. P. Yao | Assistant Manager, Battery Program |
| J. E. Battles | Group Leader, Materials Development |
| A. A. Chilenskas | Group Leader, Battery Design |
| E. C. Gay | Group Leader, Cell Fabrication |
| R. K. Steunenberg | Group Leader, Cell Chemistry |
| W. J. Walsh | Group Leader, Advanced Cell Engineering |

May 1976

Previous Reports in this Series

| | |
|---|---|
| ANL-8109 | January—June 1974 |
| ANL-75-1 | July—December 1974 |
| ANL-75-36 | January—June 1975 |
| ANL-76-9 | July—December 1975 |

# FOREWORD

Argonne National Laboratory's program on high-temperature secondary batteries is carried out principally in the Chemical Engineering Division, with assistance on specific problems being given by the Materials Science Division and, from time to time, by other Argonne divisions. The individual efforts of many scientists and technicians are essential to the success of the program, and recognition of these efforts is reflected in the individual contributions cited throughout the report.

TABLE OF CONTENTS

LIST OF FIGURES

LIST OF TABLES

# HIGH-PERFORMANCE BATTERIES FOR OFF-PEAK ENERGY STORAGE AND ELECTRIC-VEHICLE PROPULSION

Progress Report for the Period
January-March 1976

## ABSTRACT

This report describes the research and management efforts of Argonne National Laboratory's program on lithium/metal sulfide batteries during the period January-March 1976. These batteries are being developed for energy storage on utility networks and for electric-vehicle propulsion. The present cells are vertically oriented, prismatic cells with a central positive electrode of FeS or $FeS_2$ and two facing negative electrodes of lithium-aluminum alloy, and an electrolyte of molten LiCl-KCl. The cell operating temperature is 400-450°C.

The program has advanced to the point where electrodes and cells, as well as other cell components, are being fabricated by several industrial firms under contracts with Argonne. These firms are also participating in development of fabrication methods that are amenable to mass-production. In this way, the technology will be available at an early date for production of batteries. The type of cell receiving major attention is one in which the electrodes are assembled in the uncharged state. The active material in the positive electrode is a mixture of $Li_2S$ and iron; the electrode is formed by hot-pressing this material with electrolyte, by loading it into a porous structure of metal, or by incorporating it into a carbon-bonded structure. The negative electrode is a porous aluminum structure, with which the lithium reacts on first charge to form a lithium-aluminum alloy. Several methods of adding excess lithium capacity to the cell are being investigated; this addition appears to be necessary for increasing the achievable capacity of the cell.

In cooperation with industrial firms, intensive efforts are being made to develop feedthroughs and electrode separators that meet performance and cost goals. Work is also being carried out on an improved design of a battery for energy storage on utility networks and on design and fabrication of other battery components, such as a system for equalizing the charge of battery cells.

In cell chemistry studies, $Li_2S$ produced by an industrial firm is being characterized in terms of purity and physical characteristics to determine its suitability for use in fabricating uncharged cells. Work is continuing on the development of alternative secondary cell systems with calcium- or magnesium-based negative electrodes and molten-salt electrolytes.

## SUMMARY


### Cell Fabrication

A procedure has been established for testing the cells fabricated by industrial firms under contract with ANL. Life testing will be conducted at the 10-hr rate and, periodically, capacity tests (at 10-, 5- and 2-hr discharge rates and 5-hr charge rate) as well as maximum-power tests will be carried out. These tests are being applied to cells that have already been received by ANL.

Two prototypes of cells to be made under the contract with Eagle-Picher were received and tested. One of these, an $FeS_2$ cell, failed at the junction between the positive terminal rod and the molybdenum current collector owing to stresses created in the positive electrode by alignment problems. Design changes to alleviate the stress are under investigation.

The first cells produced under the contract with Gould Inc. have been received; these cells are made with porous current collectors and powders of active materials. Because of problems with the porous material from which the negative electrodes were made, the specific energy of these cells is only 60 W-hr/kg. One cell was operated for 870 hr and 38 cycles before the test was terminated.

Carbon-bonded positive electrodes continue to show good performance and cycle life characteristics. Present effort is centered on setting specifications for cells to be produced under future contracts. Cell KK-3, a carbon-bonded, uncharged $FeS_2$ cell designed for operation on the upper voltage plateau has demonstrated a high specific power of 100 W/kg. Operation of this cell led to development of an improved fabrication technique. Cell KK-4, a charged, upper-plateau $FeS_2$ cell, has attained a specific energy of 80 W-hr/kg. Both KK-3 and KK-4 have exhibited very stable discharge capacities at current densities up to 0.10 $A/cm^2$. Cell KK-5, an uncharged FeS cell that is undergoing start-up testing, has a cell resistance of only 4 $m\Omega$; this low resistance demonstrates the progress that is being made in cell design and fabrication techniques.

### Materials Development

Various prototype feedthroughs, received as a result of the on-going development programs by several commercial feedthrough manufacturers, were tested. The results to date indicate that at charge cutoff potentials greater than 1.8 volts the niobium-base brazes developed by ILC Technology fail in unsatisfactorily short times. Failure is due to the bridging across the ceramic insulators by niobium metal to form a conductive path between the two electrodes. Studies were conducted to determine the strength of pressed and sintered $Y_2O_3$. The data from four-point bend tests suggest that the strength of $Y_2O_3$ bars is maximized at 94% theoretical density with ultimate strengths limited to the 110-120 $MN/m^2$ range. Preliminary tests of $Y_2O_3$-based mixed oxide bodies with MgO or $Al_2O_3$ additives indicate that even higher flexual strengths are obtainable. A characterization program for paper and felt separators was instituted. A test cell was designed specifically for testing paper separators and the first cell has operated over 500 hr

with an yttria-asbestos composite separator. Several papers and felts have recently been developed which look very promising.

Static corrosion tests have been used to evaluate the corrosion resistance of several metals and alloys in both FeS and $FeS_2$ environments. For materials that have been tested over the 400 to 500°C temperature range, the corrosion rate is increased by roughly an order of magnitude at the higher temperature. The higher temperatures also promote the formation of partially adherent sulfide reaction layers on molybdenum and molybdenum-bearing alloys. Examinations were conducted on prismatic cells S-81, S-83, and S-85 which utilized macroporous vitreous carbon current collectors in the compartmentalized positive electrodes. Examinations showed that the regions immediately below the partitions were void of electrolyte and active material. Although the electrochemically formed Li-Al electrode from Cell S-83 was one of the more uniformly reacted electrodes, the distribution of material was nonuniform with the volume fraction of Li-Al ranging from 0.17 to 0.58.

Postoperative examinations were conducted on cells fabricated under industrial contracts with Gould Inc. and Eagle-Picher Industries. In each cell, the molybdenum sheet current collector had fractured at the spot-welded junction to the molybdenum rod conductor. The electrical shorts that developed in the Gould cell have been attributed to the presence of carbon cement particles within the BN separator.

Battery Design

Lithium requirements for off-peak energy storage on electric utilities and electric vehicle propulsion have been estimated for the period 1985-2000. The annual requirements are expected to rise from $2.2 \times 10^6$ kg in 1985 to $1.2 \times 10^8$ kg in 2000. Cumulative requirements would reach $9.3 \times 10^8$ kg by 2000. This projected requirement represents a substantial fraction of present estimates of world lithium resources and is nearly equal to estimated U. S. recources that are economically recoverable. Expansion of both exploration and production capacity will be needed if lithium requirements for Li-Al/$FeS_x$ batteries are to be met.

Design studies are being continued to establish cell and battery specifications for a 200 MW-hr utility energy storage system. A modular design is being investigated which is based upon a truckable module of 5500 kW-hr capacity. Each module contains 90 cells connected in parallel. Six modules are connected in series to form a string, and six strings make up the battery. Calculations of heat removal rates and insulation performance show that desired temperature control can be achieved during a 10-hr discharge for load leveling. Further calculations are being made to evaluate means for controlling temperatures during more rapid discharges, such as those required for peaking application.

A contract was completed with an outside vendor to fabricate 26 cell-cycler modules for the cell and battery testing program. A protective circuit for the system was also designed and installed on an existing cell cycler for testing. A four-cell charge-equalization system was successfully demonstrated and a preliminary design was completed of a prototype six-cell charge-equalizer system suitable for use on an electric vehicle. Testing of

lithium-aluminum/iron sulfide cells in series and parallel arrangements has begun in non-glovebox facilities. Contractor-fabricated cells are being used for this testing.

Industrial Contracts

An addendum to the contract with Gould to develop, fabricate, and test uncharged cells with hot-pressed positive electrodes became effective March 1, 1976. Prototype cold-pressed FeS and $FeS_2$ cells were delivered by Eagle-Picher and were evaluated. Approval to proceed with the FeS cells was given to Eagle-Picher.

Tests of several methods of fabricating felt-type BN separators with a BN binder are encouraging. Development and testing of a felt-type separator made of $Y_2O_3$, which promises lower costs, are also being pursued.

Prototype ram-type and brazed-type feedthroughs have been received and are being evaluated. Work on development of a nonmetallic braze for a $Y_2O_3$ insulated feedthrough has begun.

A promising method of producing low-cost $Li_2S$ powder has been reviewed with several potential suppliers.

A preliminary design of a low-cost cell equalization/charger has been completed.

Cell Chemistry

A Li-Al/$FeS_2$ cell was operated with a porous Fe-Mo-Ni current collector in the $FeS_2$ electrode. The electrical performance of the cell was excellent; the coulombic efficiency was greater than 95% and utilization of the $FeS_2$ was greater than 80%. Post-test evaluations are being made to determine whether the current collector was subject to significant corrosive attack.

Because of the present interest in Li-Al/$FeS_x$ cells fabricated in the uncharged state, the availability of high quality $Li_2S$ has assumed increased importance. Two lots of material prepared by Eagle-Picher Industries, Inc. by a new procedure involving the reaction of $Li_2CO_3$ with $H_2S$ at 700-800°C were characterized by chemical analyses, metallographic examination and X-ray diffraction. Both lots appear to be of reasonably high purity and appear to have suitable physical properties for use in cells.

A study was conducted on the addition of 10 at. % potassium ions to LiF-LiCl-LiBr electrolyte to determine whether the liquidus temperature would be lowered sufficiently below the value of 445°C to make the system suitable for use as an electrolyte in Li-Al/$FeS_x$ cells. Although a significant decrease in the liquidus temperature was observed, the phase relationships of the modified system are not favorable for cell use.

Further investigations on the wetting characteristics of molten LiCl-KCl were made on stainless steel solid surfaces, stainless steel screen, and boron nitride paper. The stainless steel was wet easily, and the boron nitride with difficulty. A large hysteresis effect between the advancing and receding contact angles was observed in all cases.

## Advanced Cell Engineering

This effort is directed primarily toward the development of advanced electrodes and cell configurations for the Li-Al/$FeS_x$ system. The development of uncharged FeS and $FeS_2$ electrodes has been continued; improvements in performance have been achieved through the addition of $Li_2C_2$ to the positive electrode. This supplemental lithium capacity prevents the cells from being limited by the negative electrodes. Other methods of providing additional lithium capacity are also under study. Several Li-Al/FeS cells have been under test for greater than 3000 hr with stable operation. An improved electrode-pressing technique was developed to allow the preparation of compact, uncharged $FeS_2$ electrodes.

Studies of alternative negative electrodes have concentrated on alloys containing lithium and silicon. A binary lithium-silicon alloy was found to be capable of higher specific energy than lithium-aluminum, but polarizations were prohibitively high, thereby preventing operation at practical discharge and charge rates. Ternary alloys of lithium and silicon with other metals are being investigated to find a high-capacity negative electrode of improved power capability.

Work is also under way on the development of a "button" cell which may be stacked in a bipolar array, and studies are being continued to determine the factors that limit the lifetime of Li-Al electrodes.

## Alternative Secondary Cell Systems

Studies of rechargeable molten-salt-electrolyte cells with calcium and magnesium negative electrodes, which are being conducted mainly on a laboratory scale, have indicated that both of these materials are promising candidates for low-cost battery systems. The negative electrodes currently under test include $CaAl_2$, $Ca_2Si$ and Mg. Positive electrodes being used in the cells are FeS, $Fe_3O_4$ and $FeS_2$. Prismatic cells using the $Ca_2Si$/FeS and $CaAl_2$/FeS couples have achieved specific energies of about 35 W-hr/kg. Efforts to improve the cell performance are in progress.

# I. INTRODUCTION

Lithium/metal sulfide batteries are being developed at Argonne National Laboratory (ANL) for use as (1) energy storage devices for load-leveling on electric utilities and (2) power sources for electric automobiles. Batteries that are currently available are too expensive for the first application and have insufficient energy storage and power per unit weight for the second application. The installation of batteries on electric utility networks would permit the utilities to store energy generated at night by coal-burning or nuclear baseload plants and discharge the battery to the network during the day when demand is highest. This would reduce the need for gas- or oil-burning turbine generators. Electric automobile batteries could be recharged at night using electricity produced from coal or nuclear energy. The successful development of batteries for either application would reduce our dependence on foreign sources of oil.

The development effort on the energy storage battery, which is funded by ERDA, includes cell chemistry studies, materials studies, electrode development, cell development, battery development, and systems studies. The development of the electric-vehicle battery, which is also funded by ERDA, consists of systems design studies and cell and battery development; most of the more basic studies performed under the energy storage battery program are also applicable to the vehicle-propulsion effort.

The performance goals that we have set for off-peak energy storage and electric-vehicle batteries are given in Table I-1. As a result of a recent reevaluation, the goals for the off-peak energy storage battery have been

Table I-1. Performance Goals for Lithium/Metal Sulfide Batteries

| Battery Goals | Electric Vehicle Propulsion | Off-Peak Energy Storage |
|---|---|---|
| Power | | |
| Peak | 60 kW[a] | 40 MW |
| Normal | 20 kW | 10 MW |
| Voltage, V | 140 | 1000 |
| Specific Energy, W-hr/kg | 120-160[b] | 80-150[b] |
| Energy Output | 40 kW-hr | 100 MW-hr |
| Discharge Time, hr | 2 | 5 |
| Charge Time, hr | 5 | 5-7 |
| Watt-Hour Efficiency, % | 70 | 80 |
| Cycle Life | 1000 | 3000 |
| Cost of Capacity, $/kW-hr | 20-30[c] | 20-30[c] |
| Heat Loss Through Insulation | 150 W | 100 kW |

[a] Based on the power required to accelerate a 1570-kg car from 0 to 50 mph in 15 sec.

[b] Includes cell weight only; insulation and supporting structure for battery would add approximately 20% to the weight.

[c] Includes cost of cells, but not battery structure and insulation.

changed from those given in the preceding semiannual report (ANL-76-9, p. 9). The lower end of the specific-energy range, a factor of only indirect importance in off-peak energy storage batteries, has been reduced from 120 to 80 W-hr/kg to permit greater flexibility in design. The discharge time has been reduced from 10 to 5 hr because of the expectation that in the near future batteries are more likely to be used for peaking purposes than as a replacement for intermediate generating capacity. The cycle life has been increased from 1500 to 3000 cycles to permit operation of the battery for a period of 8 to 10 yr before replacement is required. The lower ratio of capacity to power and the longer cycle life would permit higher costs for the battery, and this consideration is reflected in the increase in the goal for cost of capacity to $20-30/kW-hr.

Development work at ANL on the Li-Al/metal sulfide cells has progressed to the stage where contracts have been made with several industrial firms to develop fabrication techniques and fabricate electrodes and cells. These contracts effectively utilize the expertise of battery manufacturers and at the same time facilitate the transfer of ANL-developed technology to industry. Contracts have also been made with several industrial firms to develop improved electrode separators and electrical feedthroughs.

As a result of the increased emphasis on commercial development, a change was made recently in the organizational structure of the program. The new format of the report reflects this change. The effort encompassing cell fabrication, materials development, and battery design is strongly oriented toward establishing the capability for commercial fabrication of Li-Al/$FeS_x$ batteries at the earliest possible date. Cell chemistry studies and advanced cell engineering studies provide support for the commercial development effort, and close cooperation among the groups is maintained. A small portion of the overall effort is directed toward investigations of promising alternative systems for secondary battery application.

# II. COMMERCIAL DEVELOPMENT OF Li-Al/METAL SULFIDE BATTERIES
(R. O. Ivins)

## A. Cell Fabrication
(E. C. Gay)

Cell fabrication efforts are directed toward developing and evaluating designs and fabrication methods that will lead to the production of cells meeting our goals for battery performance. In this effort, a strong emphasis is placed on suitability for large-volume production. These designs and methods are further developed by industrial firms under contracts with ANL, and contractor-produced cells are tested and evaluated at ANL.

### 1. Development and Testing of Contractor-Produced Cells
(W. E. Miller)

#### a. Testing Procedure
(R. C. Elliott, T. O. Cooper)

A procedure for testing Li-Al/$FeS_x$ cells fabricated by industrial contractors is being devised and implemented. Establishment of such a testing procedure among all the contractors and ANL will standardize the data-analysis task. It will also provide information on cell performance so that various designs may be compared with each other and with our performance goals. The procedure and test conditions are outlined below.

All cells will be tested at 430°C ± 10°C. The cutoff voltages (IR-included) with $FeS_2$-type cells will be 1.95 V for charge and 0.9 V for discharge; with FeS-type cells, 1.62 V, charge and 1.0 V, discharge. Life tests will be conducted at charge and discharge rates of 10 hr. Initially and at every 500 hr during the life tests, cells will be subjected to capacity and power capability tests. Discharge capacity will be measured for the 5- and 2-hr rates at intervals over the 500-hr period, and charge capacity will be measured at the 5-hr rate every 500 hr. Power capability will be determined from four 15-sec discharge power pulses which have been selected to bracket the cell maximum power; these measurements will be made at full charge and at 50% discharge. Test measurements of this type are described in Section A.1.c. below.

#### b. Gould Cells
(R. C. Elliott, T. O. Cooper)

The first Li-Al/$FeS_x$ cells built under industrial contracts were received from Gould in mid-November 1975. These cells have positive electrode current collector structures of vitreous carbon foam infiltrated with $FeS_x$ powder, and negative electrodes of porous iron infiltrated with Li-Al powder. Details of the cell construction were given in the preceding report (ANL-76-9, p. 73).

A number of problems were encountered in the fabrication of these cells, and these have become apparent from their operation. Because of a strike, Gould was unable to obtain the porous iron Retimet* originally

*Manufactured by Dunlop, Ltd., England.

specified, and a substitute material was used. This material was inferior to Retimet in that the pore structure limited the amount of Li-Al powder that could be loaded into the porous structure. The packing fraction of solids in the pores was limited to 0.48 instead of the expected 0.7, and the specific energy of these cells was thereby reduced from the expected value of 90 W-hr/kg to about 60 W-hr/kg. Another problem was encountered in handling the BN fabric separator. The design required considerable hand-working of the rather fragile BN to place it in a frame structure around the positive electrode. The BN separator tended to fray during this operation. This problem has shown up in cell operation where these cells have shown a tendency to short out. The shorting has sometimes been caused by particle penetration through the separator. The connection between the positive terminal of the cell and the molybdenum current collector has also caused difficulties. This problem is discussed later in Sections A.1.d and B.5.b.

One Gould cell (2-003) was operated for 870 hr and 38 cycles. The test was terminated when the cycler equipment malfunctioned and overcharged the cell. The cell achieved discharge capacities of 68-70 A-hr, or 67% utilization of the Li-Al (the limiting reactant). The ampere-hour and watt-hour efficiencies were 98 and 84%, respectively, and the specific energy was 60 W-hr/kg.

c. Eagle-Picher Cells
(R. C. Elliott, T. O. Cooper)

The cells being built under this contract have electrodes made by cold-pressing active powders. Four cells (two $FeS_2$-type and two FeS-type) have been received from Eagle-Picher. These cells were of a design that Eagle-Picher proposed under the contract, and they were submitted to ANL for evaluation of the design prior to fulfillment of the contract. The $FeS_2$ cells have square (12.7 by 12.7 cm) electrodes of the thin type (approximately 0.32 cm thick for both the negative electrode and positive electrode halves); the overall cell thickness is about 2.2 cm. Both positive and negative electrodes were made by cold-pressing powdered active materials into honeycomb current collector structures. The capacities of the cells are about 70 A-hr, limited by the Li-Al.

When Eagle-Picher completed fabrication of the two $FeS_2$ cells, the cells were radiographed. In Cell 2B2, they found a broken connection between the positive terminal rod and the molybdenum backing sheet between the positive electrode halves. The joint between the rod and the molybdenum sheet was made by slightly extending the molybdenum sheet beyond the pressed electrode (a tab-type extension was provided on the sheet); the terminal rod was then riveted and welded to the sheet. When we received the two cells, our radiograph confirmed the broken connection. The break appears to be a transverse fracture through the rod.

The second $FeS_2$ cell was tested at ANL. The cell was operated for four cycles at a charge-discharge current density of 0.025 A/cm$^2$ (10-hr rate) with the Li-Al utilization reaching 74% for the 5th discharge cycle. The overall ampere-hour efficiency for the first four cycles was greater than 99%. On the 5th charge cycle (and subsequent charges) the cell would accept a charge equivalent to only about 17% utilization; however, the ampere-hour efficiency remained high. After 19 cycles, the cell test was terminated.

Post-test examination of this cell showed a crack in the molybdenum sheet around the weld connecting the positive rod terminal to the current collector. In the remainder of the cells under the present contract, the current collector will be welded to a terminal rod that is enlarged at the joint and is made of HT grade molybdenum (a more easily welded form of molybdenum; Schwarzkopf Development Corp.).

An FeS cell (1B2) with thick positive electrodes (0.64 cm) of the Eagle-Picher design was received. The cell was tested by the procedure outlined above. The charge and discharge curves are presented in Fig. II-1, where the rate is plotted against the specific energy or specific capacity. The rather sharp decrease in capacity with decreasing hourly rate of charge or discharge was expected for thick FeS electrodes.

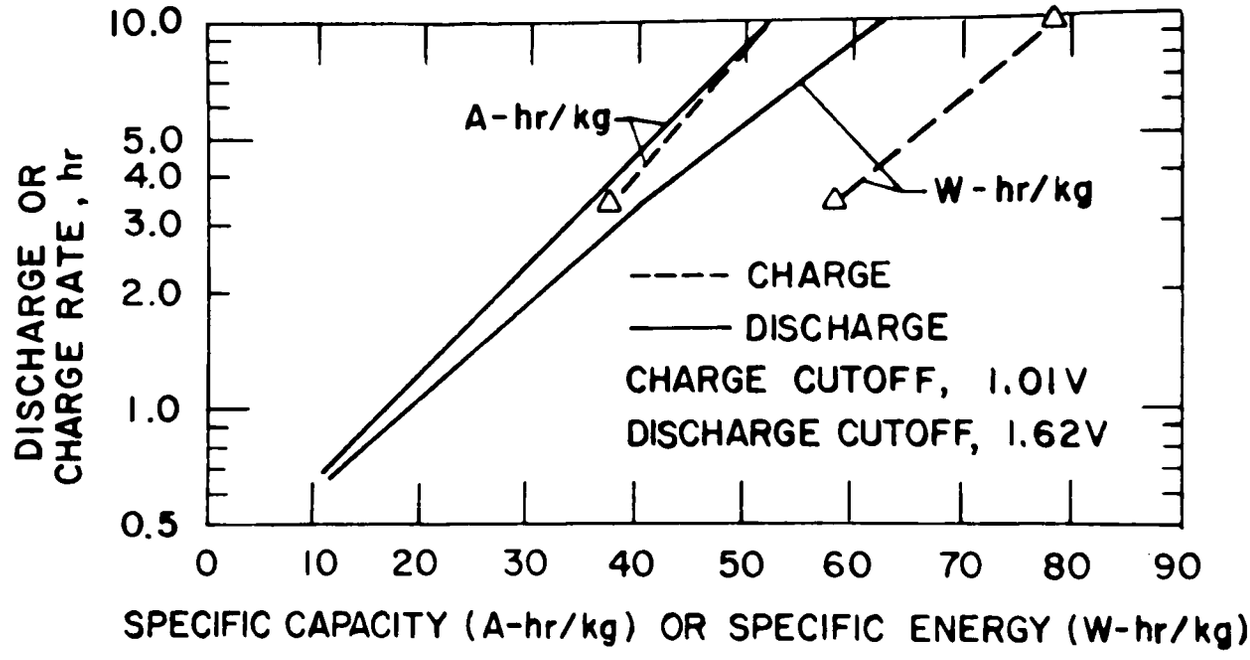


Fig. II-1. Capacity Test for Cell 1B2
(cell weight, 2.1 kg)

Power capability tests were made for Cell 1B2. These tests allowed some conclusions regarding the chemistry and mechanical design to be drawn from application of the data to a simple model of a cell. The power capability test is a modification of the "power ramp" test that has been in use at ANL for some time. Four or five 15-sec high-current pulses are drawn (with capacity replacement) at full charge and 50% discharge. These data are shown in Fig. II-2, as a plot of current *vs.* specific power. Application of a simple series-parallel model (also shown in Fig. II-2) results in the following equation, which may be fitted by standard regression techniques:

$$PWR = b_o + b_1\ AMPS + b_2\ (AMPS)^2$$

The terms of the equation are defined as follows:

$b_o$ is the shorting power, *i.e.*, the rate of energy loss in watts with no cell current being drawn externally, or the power due to the internal shorting current through $R_p$. E is an ideal voltage. Normally, $b_o$ is negative and very close to zero.

$b_1$ is the value of E, the ideal voltage. E and AMP are positive.

$b_2$ is the cell internal resistance in ohms. This item represents the "$I^2R$" losses due to $R_s$ and is negative.

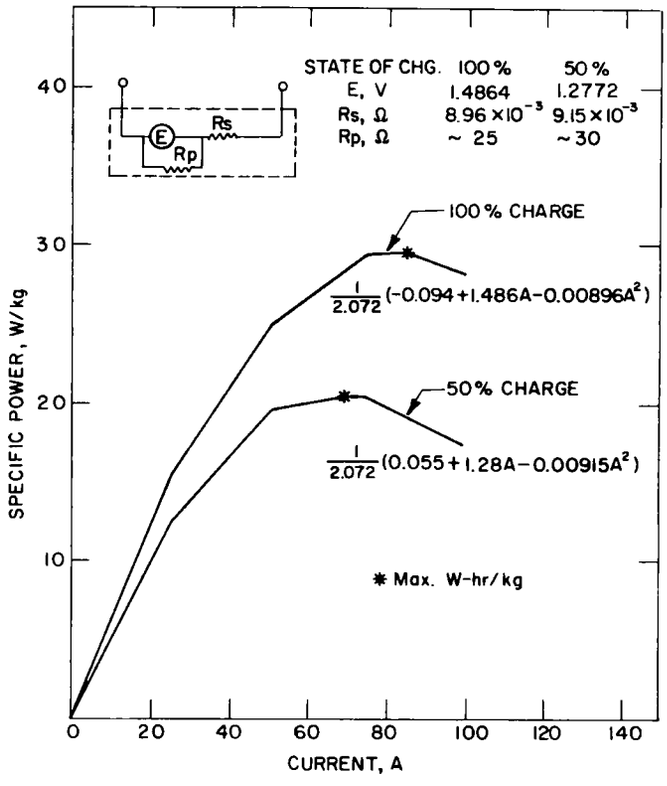


Fig. II-2. Power Capability of Cell 1B2

The data from Cell 1B2 were fitted to the model by computer. The resulting parameters are also indicated in Fig. II-2. Correlation coefficients were >0.999, indicating a high degree of confidence in the model as applied to these data. These tests will be repeated every 500 hr throughout the cell lifetime to gain information on variation of the data with time.

### d. Molybdenum Current Collectors for $FeS_2$ Cells
(T. O. Cooper)

The problem of making a suitable joint between the positive terminal and the current collector may be attributed to design weaknesses in the prismatic cell. The positive-electrode terminal rod is rigidly attached to both the feedthrough and the positive electrode over a relatively short distance within the cell. Consequently, a slight misalignment of the rod can cause stresses within the positive electrode which, in turn, can exert forces on the separator; the end result can be a short in the cell or, in the case of $FeS_2$ cells in which the welded molybdenum has recrystallized,

a break in the molybdenum. As a possible solution to these problems, we are undertaking the development of current collectors and internal cell connections made from molybdenum wires.

One such design is shown in Fig. II-3; in this design, molybdenum wire is wound on an iron mandrel to form the current collector. Iron is a suitable material for the mandrel because a sheet 0.025 cm thick or less comprises less than 10% of the iron used in the positive electrode of an $FeS_2$ cell. Fine molybdenum wire (5-20 mil diameter) can be handled in the manner shown. The square mandrel sheet is notched on three of its edges. One continuous wire filament is wound through the notch, through the snap ring at the top of the sheet, over a yoke at the top, back through the snap ring on the opposite side of the sheet, and then through the next notch in the mandrel. This procedure is continued until all the notches have been filled. The snap ring is then compressed to secure the wire and the yoke is removed and discarded. The wire loops are bundled together at the top, a BN insulating tube is placed over the bundle, and then a long metal cap is silver-brazed to the wire bundle. Thus, the braze is at the top of the positive terminal and corrosion should be minimal. An electrode can then be made by the usual technique of pressing the mixture of active material and electrolyte onto the wound mandrel sheet to give an electrode with a flexible joint between the positive electrode and the feedthrough. This technique will be evaluated in future cells operated at ANL.

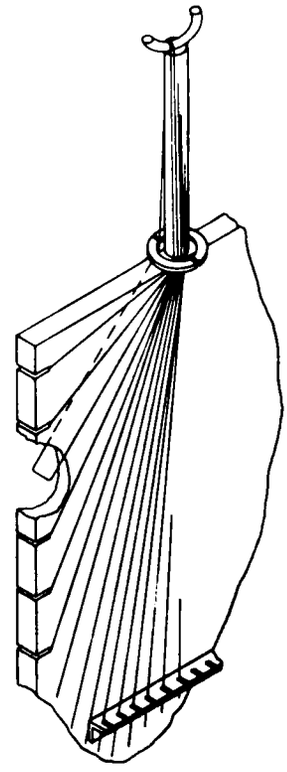

Fig. II-3. Fine-Wire Molybdenum Current Collector

## 2. Macroporous Bonded Positive Electrodes
(T. D. Kaun)

A carbon-bonded positive electrode structure formed from a paste of carbon binder, active electrode material, and a volatile (ammonium carbonate) gives an electrode of controlled porosity. After a 400°C cure, the electrode consists of evenly dispersed particles of active material held in a carbon lattice. The carbon binder (National, grade C-34) has proved to be compatible with all present types of positive electrodes, both charged and uncharged. Electrode tests with a variety of positive electrode materials ($Li_2S$, $FeS_2$, FeS, $CoS_2$, $Cu_2S$) all have shown that the carbon-bonded electrode shows very good utilization and cycle life characteristics (ANL-76-9, p. 24).

The advantages of easy and low-cost fabrication have made the carbon-bonded electrode a prime candidate for contractor-fabricated cells. Present carbon-bonded electrode fabrication involves the spreading or packing of a paste containing the active material into a metal current collector tray (Mo with $FeS_2$ and Fe with FeS); the current collector tray of a typical cell (KK-4) is shown in Fig. II-4a and the completed electrode in Fig. II-4b. The electrode is faced with a particle retainer of zirconia fabric. After a curing at 100°C for 8 hr and at 400°C for 8 hr between 0.32-cm-thick steel plates, a unified structure is formed with zirconia fabric bonded to the electrode face. With this technique, active material loading (A-hr/cm$^3$), electrode void volume, and electrode thickness can be easily varied and easily controlled. Although development of the carbon-bonded electrode is being actively pursued, more work is needed before this type of electrode is incorporated into contractor-produced cells. The effort described below has been concentrated on setting specifications and developing cell designs for future contractor-fabricated cells.

Three compact, prismatic cells (12.7 cm x 12.7 cm) using carbon-bonded positive electrodes were fabricated and operated. The pertinent physical characteristics and cell performances can be found in Table II-1. These cells were operated at 450°C using LiCl-KCl eutectic electrolyte (from Lithcoa, filtered before use). A BN fabric separator and zirconia fabric particle retainers were used for both negative and positive electrodes in all cells. Care in design and fabrication of the metal electrode current collector has enabled the cell resistance to be reduced to 4 mΩ.

Cell KK-3, an upper-plateau $FeS_2$ cell, was the first cell having a carbon-bonded, uncharged positive electrode. During curing, some swelling of the low-porosity (10-15%) carbon-bonded electrode occurred, thereby reducing the active material loading (A-hr/cm$^3$). The technique was later improved by curing the electrode between restraining plates. In operation, the cell was unrestrained and exhibited no swelling. The capacity of Cell KK-3 was somewhat lower than expected (35 A-hr or 50% of theoretical instead of the expected 60%). The discharge capacity was very stable at 35 A-hr for current densities of 0.025 to 0.10 A/cm$^2$ (7.5 to 30 A). For 15-sec power pulses, the specific power was 100 W/kg at full charge and 60 W/kg at 50% discharge. The cell was operated for 80 cycles and 1100 hr, when operation was terminated because of an equipment failure.

Cell KK-4, a charged, upper-plateau $FeS_2$ cell, has a specific energy of 80 W-hr/kg. The discharge capacity is 90 A-hr, which was the designed

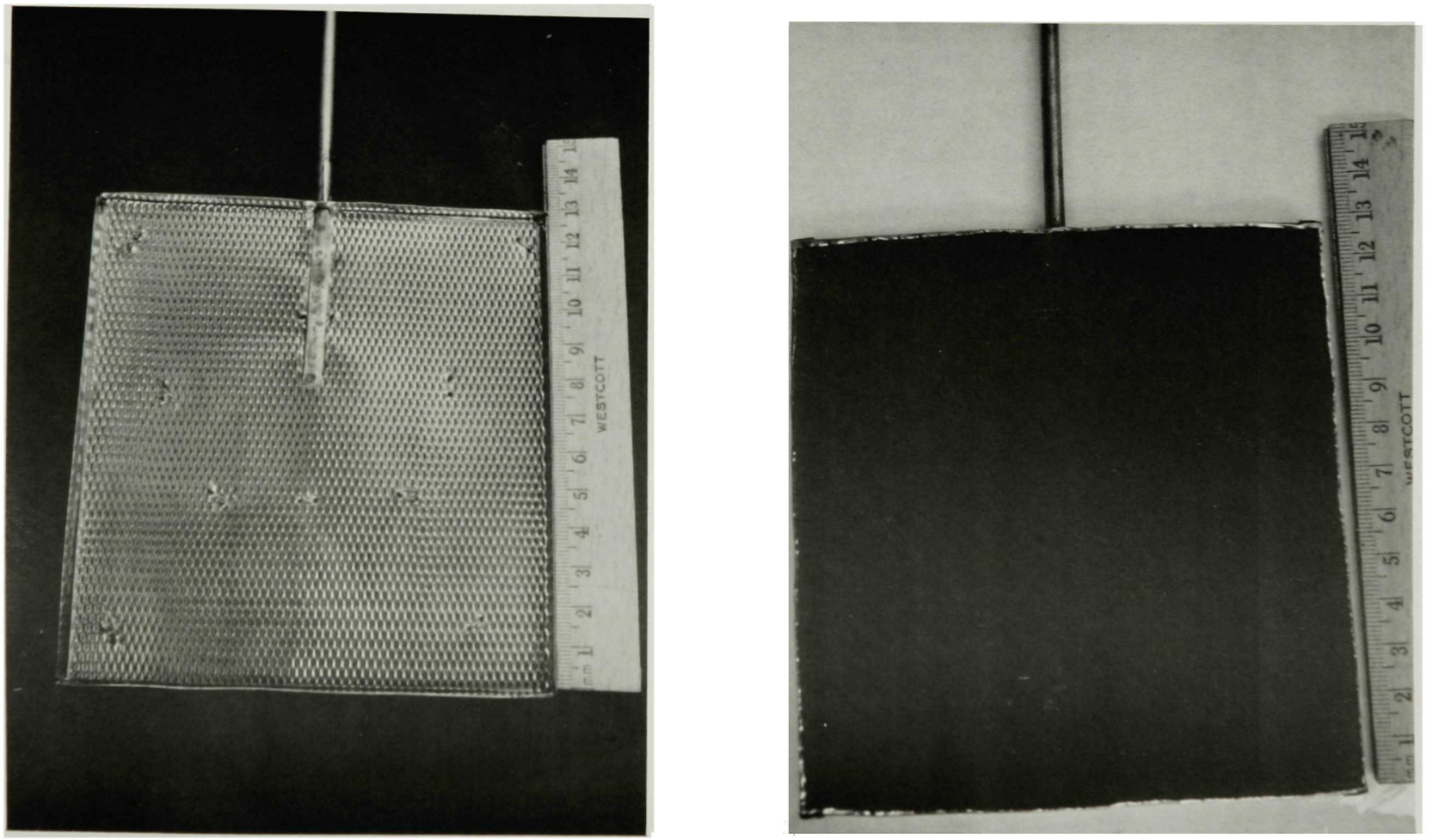


Fig. II-4. Construction of Carbon-Bonded Positive Electrode of Cell KK-4

a. Molybdenum current collector tray faced with molybdenum mesh. Rod is attached by Hastelloy B brazing and molybdenum riveting.

b. Completed carbon-bonded positive electrode with zirconia fabric bonded to the face. Total thickness of electrode compact is 8 mm; capacity is 180 A-hr of $FeS_2$-$CoS_2$.

Table II-1. Performance of Cells with Carbon-Bonded Electrodes

| | Cell KK-3 | Cell KK-4 | Cell KK-5 |
|---|---|---|---|
| Type of Cell | Upper-plateau $FeS_2$, uncharged | Upper-plateau $FeS_2$, charged | FeS, uncharged |
| Positive Electrode[a] | 60% $Li_2S$, 25% $FeS_2$, 15% $CoS_2$ | 85% $FeS_2$, 15% $CoS_2$ | 100% $Li_2S$ |
| Loading, A-hr/cm$^3$ | 1.2 | 2.0 | 0.9 |
| Theo. Capacity, A-hr | 115 | 180 | 120 |
| Negative Electrode | Al wire | Hot-pressed Li-Al | Al wire, hot-pressed Li-Al |
| Loading, A-hr/cm$^3$ | (1 g Al/cm$^3$) | 0.9 | 0.9 |
| Theo. Capacity, A-hr | 70 | 150 | 180 |
| Performance | | | |
| Hours | 1100 | >900 | >50 |
| Cycles | 80 | >5 | >3 |
| % Utilization | 50[b] | 60[b] | 75[c] |
| A-hr Efficiency, % | 93 | 98 | - |
| W-hr Efficiency, % | 79 | 82 | - |
| Cell Resistance, mΩ | ∿5 | ∿6 | 4 |
| Measured Specific Energy, W-hr/kg | 42 | 80 | >60 |

[a]Values represent the percent of theoretical capacity supplied by each constituent; the ratio of active materials in Cell KK-3 provided a higher A-hr/cm$^3$ loading than could be achieved with $Li_2S$ alone.

[b]Capacity of cell limited by the negative electrode.

[c]Capacity of cell limited by positive electrode.

upper-plateau capacity. This capacity is stable at the 10- and 5-hr discharge rates (current densities of 0.035 and 0.070 A/cm$^2$). The performance of Cell KK-4 strongly suggests that the specific energy goal of 100 W-hr/kg can be achieved with the present technology in cells with carbon-bonded positive electrodes. The hot-pressed Li-Al negative electrodes used have not performed as well as desired, and some improvements in performance will be sought. After 50 cycles and 900 hr, Cell KK-4 continues to operate with good efficiency and capacity.

Cell KK-5, an uncharged FeS cell, was fabricated with excess negative electrode capacity. A hot-pressed Li-Al plaque was incorporated with the aluminum wire plaque. The carbon-bonded positive electrode was fabricated using $Li_2S$, Fe, and Cu; with improved techniques, a loading of 0.9 A-hr/cm$^3$ was achieved. The main difficulty in attaining high positive-electrode loadings with uncharged cells is due to the low bulk density of $Li_2S$.

Calculations of the active material loadings of carbon-bonded and hot-pressed electrodes has brought insight into methods of improving these fabrication techniques. Similar loadings are achieved in both types of

positive electrodes, as shown in Table II-2. The specification of 70 vol % active material in the discharged state appears necessary for achieving high specific energy. The low bulk density of $Li_2S$ creates problems in attaining the desired loadings for all types of uncharged electrodes. In the fabrication of carbon-bonded electrodes, the closed pore volume is included in the designed void volume. In hot-pressing without vacuum, pore gas is trapped by the liquid salt and compressed. Calculations have indicated that the volume percent carbon is comparable to the volume of trapped gases of pressed electrodes. Therefore, it is understandable that similar electrode loadings can be obtained by the two techniques. Higher loadings could be obtained by both methods by the use of higher bulk density $Li_2S$; similar results could be obtained in carbon-bonding by the use of a lower volume of carbon and in hot-pressing, by an increase in pressure.

Table II-2. Comparison of Positive-Electrode Loadings by Two Techniques

| Electrode Composition, % of Theor. Capacity | Max. Loading of Active Material,[a] A-hr/cm$^3$ | Loading Achieved, A-hr/cm$^3$ | |
|---|---|---|---|
| | | Carbon-Bonded Electrode | Pressed Electrode |
| 50 $Li_2S$-35 $FeS_2$-15 $CoS_2$ | 1.17 | 1.2 | - |
| 85 $Li_2S$-15 $CoS_2$ | 1.4 | 1.0 | 1.1 |
| 85 $FeS_2$-15 $CoS_2$ | 1.7 | 1.7 | 1.2 |
| 85 $Li_2S$-15 $Cu_2S$ | 1.1 | 1.0 | 0.8 |
| 85 FeS-15 $Cu_2S$ | 1.1 | 1.1 | 0.75 |

[a]Assumed 70 vol % active material in discharged state; the remaining volume was occupied by electrolyte and current collector.

Performance results of the achievable capacities of cells fabricated by various techniques indicates that excess lithium capacity appears necessary for good utilization. Usually cells with negative electrode capacities that are about 150% of the design capacity of the positive electrode have performed well. In uncharged cells, the amount of lithium supplied by the $Li_2S$ limits the negative electrode capacity. To attain the appropriate capacity, the negative electrode must be partially charged initially or the positive electrode must contain an additional source of lithium. The latter method is advantageous because problems of handling Li-Al alloy during fabrication are eliminated. One method of providing excess lithium is the addition of lithium carbide to the positive electrode, and the feasibility of this approach has been demonstrated (see Section V, below). Accordingly, future work on the carbon-bonding technique will include studies of uncharged positive electrodes containing lithium carbide. Future work will also include tests of carbides in bonded negative electrodes (the feasibility of carbon-bonded negative electrodes has been demonstrated in small-scale cells). Metal carbides would increase the conductivity of the bonded matrix and reduce the possibility of lithium take-up by carbon.

## B. Materials Development
(J. E. Battles)

### 1. Electrical Feedthrough Development
(K. M. Myles, J. L. Settle)

An electrical feedthrough is required in lithium-aluminum/metal sulfide cells to insulate the positive electrode conductor from the cell housing, and to seal the cell. The harsh chemical environment within the cell precludes the ready adaptation of commercially available feedthroughs; the few that are resistant to the environment do not meet requirements such as leak-tightness, compactness, and low cost.

As reported in ANL-76-9, p. 36, several commercial vendors have produced feedthroughs under development contracts with ANL. Recent effort has concentrated on testing and evaluating these feedthroughs, particularly those produced by ILC Technology, in which BeO, $Al_2O_3$, or Lucalox ceramic parts were brazed with either Nb-Ni, Nb-Cu, Nb-Au, Nb-Ag, or Ni-Zr onto niobium or nickel parts. In these tests the feedthrough is sealed into a Li-Al/LiCl-KCl half-cell and a constant electrical potential is applied across the positive-electrode conductor and housing, which is at the negative electrode potential. These conditions simulate those to which a feedthrough is subjected during the charge cycle of a cell. Tests thus far have been conducted at potentials of 2.0 and 1.8 V (*vs.* Li-Al). The current through the cell is measured to determine the change in resistance across ceramic insulators with time. The as-received feedthroughs had resistances of about $10^9$ ohms at room temperature; at 450°C in a helium atmosphere, the resistances were about $10^8$ ohms. As the test progressed, the resistance of a feedthrough steadily decreased to about 1 ohm, whereupon the feedthrough failed and fell apart. Upon examination after each test, it was noted that all of the feedthroughs had formed a metallic bridge across the insulators. The principal migrating element in four of the tests was identified by spectrochemical analyses* as niobium. All of the feedthroughs failed in less than 75 hr except those brazed with nickel, which had lifetimes up to 200 hr. It should be noted that these tests are very severe and, thus, the results represent highly accelerated failures. For example, in an operating $FeS_2$-type cell, the charging potential is above 1.8 V for only about 5% of the time; thus, lifetimes of 200 and 75 hr in these tests represent cell lifetimes of 4000 and 1500 hr, respectively. Work will continue on the development of feedthroughs with braze-ceramic combinations that demonstrate reasonable lifetimes. The tests described above will also provide a clearer understanding of failure mechanisms and thus will be an aid in designing future brazed-type feedthroughs.

### 2. Ceramic Insulator Development
(W. D. Tuohig, J. T. Dusek)**

Yttria is a candidate ceramic for battery insulator applications because of its outstanding resistance to degradation by the cell environment. Specimens in the form of rectangular bars (0.5 by 0.4 by 5 cm) were prepared

*Performed by J. P. Faris, Analytical Chemistry Laboratory.

**Materials Science Division, ANL.

by die-pressing and sintering pure (99.99%) $Y_2O_3$ powder.* Fabrication parameters, such as binder concentration, compaction pressure, quantity of solvent added to plasticize the mix, size and size distribution of granules, and sintering temperature, were varied systematically to assess the influence of processing on fracture strength and microstructure. The specimens selected for testing were between 91 and 97% of theoretical density. Flexural strength data were obtained by loading the bars to failure in a four-point bend apparatus. Inner load points were 0.635 cm apart; outer points, 3.175 cm apart. The load was applied by an Instron Universal Test Machine at a uniform crosshead speed of 0.02 cm/min. The stress is calculated from the elastic beam equation according to

$$\sigma_{fracture} = 3.81 \frac{W}{bh^2}$$

where W is the load (kg), b is the beam width (cm), and h is the thickness (cm). Specimens were finish-ground to a dimensional tolerance of $\pm 1.2 \times 10^{-3}$ cm. No statistically significant difference was observed between specimens finish-ground on 600-grit SiC and those polished to an 8-μm diamond finish.

The results of the tests are summarized in Fig. II-5, which shows the average flexural strength as a function of density, and also the number of specimens in each density increment. Analysis of the data is still in progress, and a second matrix of specimens is planned. However, the present results indicate the following:

*Molybdenum Corp. of America, Louriers, Colorado.

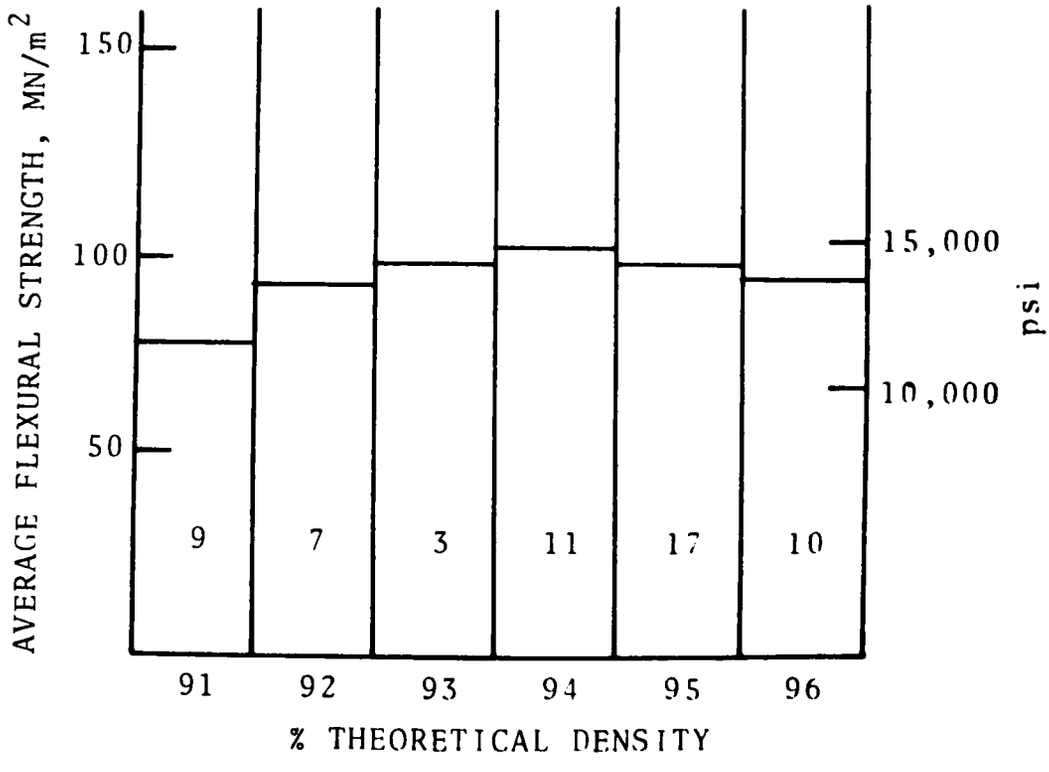


Fig. II-5. Average Flexural Strength *vs.* Density (the number of specimens tested at each density increment is indicated)

(1) Strength values of this material agree very well with the data reported by Anderson and Barker[1] for fully dense $Y_2O_3$ doped with $ThO_2$.

(2) The average measured strength appears to maximize at about 94% of theoretical density. At higher densities, strengths decrease as the result of discontinuous grain growth in the absence of an inhibitor such as $ThO_2$.[1]

(3) Fabrication flaws similar to those described previously (ANL-75-36) have been identified as the fracture origin in several of the specimens thus far examined. A detailed study of fracture surfaces of $Y_2O_3$ is planned to correlate fracture stress and flaw character. A similar study of a commercial $Al_2O_3$ ceramic established the importance of flaw characterization in the statistical analysis of brittle fracture data.[2]

(4) Ultimate strengths appear limited to about 110-120 $MN/m^2$ (16,500 psi) in pure material, although a large number of sibling specimens will be necessary to establish the 95% confidence limits.

(5) Dramatic improvement of the pressing characteristics and an increase in fired density is observed if the powder is plasticized by solvent addition prior to compaction. The drying procedure will be altered to retain a residual solvent level.

The $Y_2O_3$-MgO and $Y_2O_3$-$Al_2O_3$ binary systems are also of interest to the present work. Both MgO and $Al_2O_3$ have substantial solid solubilities in cubic $Y_2O_3$ and are "model" systems for a study of the effects of a second cation on the lithium compatibility of a stable host matrix. Magnesium oxide (MgO), in the pure state, is marginally compatible with lithium, whereas pure $Al_2O_3$ is rapidly attacked.

With increased additions of MgO or $Al_2O_3$ to $Y_2O_3$, congruently melting compounds ($Y_3Al_5O_{12}$ and $Mg_3Y_2O_6$) are formed which divide the binary phase diagrams. If compatibility can be demonstrated for these compounds, all compositions having greater $Y_2O_3$ content than the above compounds are of potential interest. Dilution of relatively expensive $Y_2O_3$ with an inexpensive, common oxide (in concentrations up to 75 mol %) would have a substantial impact on the projected cost of ceramic components. Moreover, preliminary results indicate that the mixed oxides are substantially stronger and more readily sintered than pure $Y_2O_3$. A 50 mol % MgO-$Y_2O_3$ mixture was milled, pressed and fired to a density of 4.48 $g/cm^3$; the flexural strength of the material was 148 $MN/m^2$ (21,500 psi). A 20 mol % $Al_2O_3$-$Y_2O_3$ mixture was prepared and sintered to 4.49 $g/cm^3$ at 1750°C, with a resulting average strength of 135 $MN/m^2$ (19,500 psi). These two compositions were selected to produce a less refractory, two-phase microstructure of cubic-$Y_2O_3$ solid solution and the congruent compound. The compatibility of both compositions with lithium will be evaluated next.

### 3. Electrode Separator Studies

(J. P. Mathers, T. W. Olszanski)

Efforts to develop low-cost separator materials that are compatible with Li-Al/metal sulfide cells are continuing. The separator cost could be reduced through the use of a fiber that is less expensive than the presently used boron nitride or by the development of paper or felt separators that

require less fiber per square foot. Yttria ($Y_2O_3$) is the only other material that is presently available in the form of fiber and has proven compatibility with lithium; these fibers are commercially available at $200/lb (BN fiber is $1056/lb). However, because of the higher density of yttria, an amount of yttria fiber equivalent to a pound of boron nitride fiber costs $520, which still represents a considerable savings. The long-range availability of yttria as a raw material is a major concern. Paper and felt separators based on both of these fibers are being developed through contracts with the University of Florida* and the Carborundum Company (see Section II.D.2, below).

An improved test facility has been set up for the characterization and testing of candidate paper and felt separators. With the test procedures that have been developed, the following properties can be accurately determined: thickness, basic weight (weight per unit area), percent porosity, burst strength (related to the tensile strength), flexibility (the smallest diameter to which the material can be bent), structure by scanning electron microscopy, ease of wetting by molten salt, and binder stability in molten salt. These test results will provide the basis for the preliminary selection of candidate separator materials, which will then be subjected to in-cell testing.

The ability to provide a realistic in-cell test for a paper or felt-type separator has been greatly improved with the design of a new Li-Al/LiCl-KCl/FeS test cell. The new cell design (Fig. II-6) is cylindrical with horizontal electrodes. The electrodes consist of FeS and Li-Al alloy powders which are vibrated into porous iron current collectors. The separator is kept under compression by the cell components, and thus the structure of the

*Prof. R. D. Walker, Chemical Engineering Department, funded directly by ERDA.

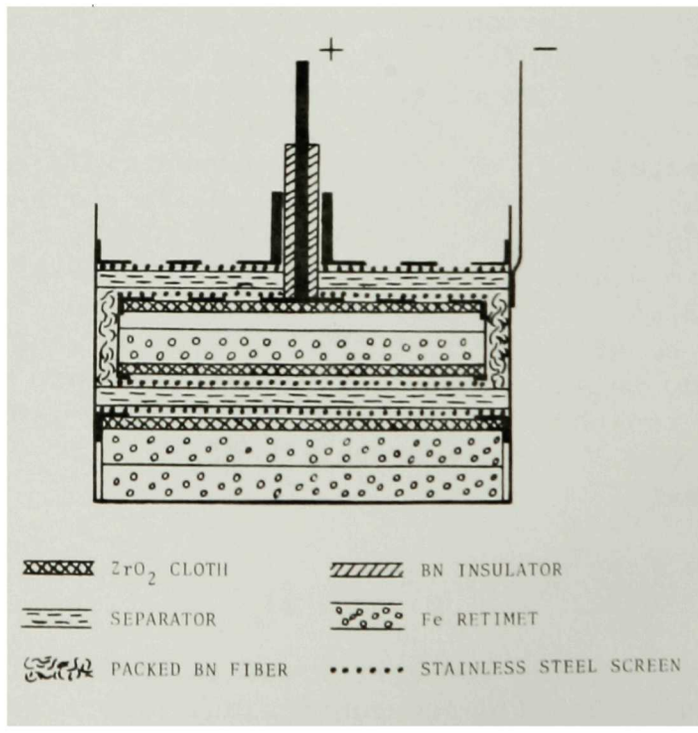


Fig. II-6. Cell for Testing Paper and Felt Separators

paper should be maintained, even if the binder used in forming the paper is destroyed by the cell environment. In previous test cells, the paper was not adequately constrained by the cell construction, and when the binder was destroyed, the paper disintegrated, thereby allowing the electrodes to short-circuit. The first test cell of this design, SC-1, utilized a yttria fiber-asbestos fiber composite paper which was developed at the University of Florida. This cell has operated over 500 hr to date with a coulombic efficiency near 100% and is slowly gaining capacity.

More recently developed papers and felts will also be tested with the new cell design. Other possible candidates for in-cell testing include composite papers with fiber combinations of yttria-asbestos, boron nitride-asbestos, and lithium aluminate-asbestos developed at the University of Florida. These papers have adequate mechanical strength for handling and assembly operations, even though asbestos fiber is unstable in the cell environment. The advantage of asbestos over organic binders is that its dissociation is not accompanied by out-gassing.

The Carborundum Company has succeeded in developing a boron nitride paper which utilizes a boron nitride binder. Although the paper is quite weak, it has sufficient strength to permit handling and is very flexible. Work is in progress to increase the density and improve the strength. The advantage of the boron nitride binder is its stability in the cell environment, which should help maintain the structure of the paper during cell operation.

In addition to these papers, an yttria felt has been developed for ANL by Zircar Products, Inc. This material is fabricated by a precursory process in which rayon felt is impregnated with $YCl_3$ and then converted to $Y_2O_3$ felt by controlled pyrolysis. The original structure of the rayon felt is retained and no binders are required. This material is easily handled and appears to be an ideal candidate for in-cell testing. The felt is presently available at $\$112/ft^2$ versus $\$515/ft^2$ for boron nitride fabric. Cost projections for larger quantities of yttria felt are as low as $\$3/ft^2$.

4. Corrosion Studies
(J. A. Smaga, J. E. Battles)

Static corrosion tests have been continued to determine the compatibility of candidate metallic materials with the positive electrode environment at temperatures of 400 to 500°C, with emphasis on corrosion resistance at the higher temperature.

The measured corrosion rates for metals and alloys that have been evaluated extensively in both FeS and $FeS_2$ environments are summarized in Table II-3. The major trend apparent from these results is the acceleration of the corrosion attack with increasing temperature; in general, the rate of reaction increases an order of magnitude or more in going from 400 to 500°C. For example, Hastelloy B (65Ni-28Mo-5Fe-1Cr) has a marginally acceptable corrosion rate in $FeS_2$ at 400°C, but this rate increases by a factor of five at 450°C, and by a factor of fifty at 500°C. Although Hastelloy C (57Ni-17Mo-16Cr-5Fe-4W) shows better corrosion resistance than Hastelloy B at 500°C in the $FeS_2$ environment, a twenty-fold increase in its corrosion rate is exhibited over the temperature range from 400-500°C. In addition to an increased

Table II-3. Materials Compatibility with the Positive Electrode Environment

| Material | Environment[a] | Corrosion Rate,[b] μm/yr 400°C | 450°C | 500°C | Remarks |
|---|---|---|---|---|---|
| Molybdenum | FeS | - | 3.0 | 10 | Minor surface attack. |
| | $FeS_2$ | 0.8 | +1.0 | +15 | Forms a weakly adherent MoS reaction layer at the higher temperatures. |
| Niobium | FeS | - | +26 | +24 | Forms an Fe-Nb reaction layer. |
| | $FeS_2$ | 770 | 2900 | >4500 | Extensive reaction. |
| Nickel | FeS | - | +7.0 | +48 | Forms an Fe-Ni reaction layer. |
| | $FeS_2$ | - | >6600 | >6600 | Complete reaction in 500 hr. |
| Hastelloy B | FeS | - | 2.5 | +11 | Localized areas of intergranular attack, weakly adherent reaction layer at 500°C. |
| | $FeS_2$ | 83 | 450 | 4000 | Nickel sulfide is the major reaction product. |
| Hastelloy C | FeS | - | 0.9 | +18 | Weakly adherent reaction layer at 500°C. |
| | $FeS_2$ | 160 | 670 | 3200 | Nickel sulfide is the major reaction product. |
| Armco Iron | FeS | 440 | 460 | 410 | Extensive intergranular attack. |

[a]Equal volume mixtures of FeS or $FeS_2$ with LiCl-KCl eutectic.

[b]Each corrosion rate listed represents an average of values from tests of 500 hr or more. Values preceded by "+" represent the formation of a reaction layer in μm/yr; those preceded by ">" represent the minimum corrosion rate based on initial sample weight.

corrodibility at elevated temperatures, niobium also exhibits embrittlement at 450°C and above. In the FeS environment, the reaction rates of all of these materials, with the exception of Armco iron, still remain acceptably low, although their corrodibility increases significantly. The high corrosion rate of Armco iron, which results from intergranular attack and consequent grain-fallout, remains relatively insensitive to temperature throughout the 400-500°C range.

Based on an acceptable corrosion of 75 μm/yr or less, a survey of the results listed in Table II-3 indicates that all the materials listed, except Armco iron, are suitable candidates for current collectors in FeS cells at temperatures to 500°C. The results also show that molybdenum is the only material suitable in both FeS and $FeS_2$ environments at 500°C; Hastelloy B shows marginal compatibility at 400°C in the $FeS_2$ environment.

### 5. Postoperative Cell Examinations
(F. C. Mrazek, J. E. Battles)

Postoperative examinations are conducted on test cells to evaluate the performance of various construction materials, in particular, feedthroughs, current collectors, electrode separators and cell housings, and to provide important information on the performance and behavior of the electrodes. During this report period, postoperative examinations were conducted on cells constructed at ANL and cells fabricated under industrial contracts with Gould and Eagle-Picher Industries. The examination procedures were described in a previous report (ANL-8109, p. 72).

#### a. ANL Cells

Cells S-81, S-83, and S-85 were operated as part of the cell fabrication effort to evaluate cells having macroporous vitreous carbon as the current collector in the positive electrode. The positive electrodes were separated into horizontal sections by graphite cloth. A summary of the physical characteristics of Cells S-81 and S-85 and the results of the postoperative examinations are presented in Table II-4. Examination of the vertical cross sections showed that the regions immediately below the partitions in the positive electrodes were void of electrolyte and active material. This condition apparently resulted from incomplete or nonuniform loading, or entrapment of gases. The concept of using graphite cloth cemented to a central sheet conductor, such as nickel, to protect against sulfide attack was tested in Cell S-85. Microscopic examination showed that the cloth was readily penetrated by the $FeS_2$ and that the nickel sheet showed severe sulfide attack.

Cell S-83 was examined primarily to determine the distribution of Li-Al within the negative electrodes. The microstructure indicated that the electrodes were uniformly utilized in most areas. Photomicrographs were taken of representative areas across the electrode thickness and were scanned by computer to determine the volume fraction of Li-Al alloy within the electrode (this procedure was described in ANL-75-36, p. 73). The volume fraction of Li-Al alloy ranged from a low value of 0.17 near the negative/positive electrode interface to a maximum of 0.58 near the center of the electrode. Because of the nonuniform distribution of Li-Al alloy, it as not possible to obtain an accurate value for the volume fraction of Li-Al for the total

Table II-4. Results of Postoperative Examinations of Prismatic Cells S-81 and S-85

| | S-81 | S-85 |
|---|---|---|
| **Cell Description** | | |
| Electrolyte | LiCl-KCl (Lithcoa) | LiCl-KCl (Lithcoa) |
| Positive Electrode | $FeS_2$-15 wt % $CoS_2$, molybdenum sheet current collector. | $FeS_2$-15 wt % $CoS_2$, nickel sheet current collector. |
| Negative Electrode | Electrochemically prepared Li-Al, 0.32 cm thick. | Electrochemically prepared Li-Al, 0.32 cm thick. |
| Operating Conditions | 1560 hr at 411-455°C. | 700 hr at ∿450°C. |
| **Postoperative Examination** | | |
| Positive Electrode | Metallographic examination: ∿3/4 of electrode was Z phase ($Li_2FeS_2$); ∿1/4, $FeS_2$. | Metallographic examination: electrode contained varying ratios of α-Fe, $Li_2S$, and X phase (approx. $Li_4Fe_2S_5$). |
| Negative Electrode | Good electrode utilization. No evidence of original wire-like structure. Thickness had doubled. | Same overall structure as S-81 except that in several locations Li-Al particulate had penetrated to contact the positive electrode. This movement of Li-Al probably caused high resistance shorting during cell operation. Thickness had more than doubled. |
| Corrosion | No apparent reaction of molybdenum current collector. | Nickel current collector severely attacked; thickness reduced from 25 to 14 mils. |

electrode; the estimated value is 0.35-0.40. Examination of the vertical cross section of the positive electrode of Cell S-83 showed void areas below the horizontal shelves similar to those observed in Cells S-81 and S-85. Also, this electrode showed definite evidence of slumping. The slumping has been tentatively attributed to the removal of the electrode from the cell housing while the electrolyte was molten.

b. Cells Fabricated under Industrial Contracts

Postoperative examinations were conducted on three prismatic Li-Al/$FeS_2$-$CoS_2$ cells fabricated by Gould Inc. (2 cells) and Eagle-Picher (1 cell). Examination of each cell showed a brittle fracture where the molybdenum conductor was joined, by rivets and spot welds, to the molybdenum current collector (see Section II.A.1). Also these cells were incompletely filled with electrolyte; the electrolyte level varied from about even with the top of the electrodes to as much as one inch below. Localized areas within the electrodes and BN fabric separator were void of electrolyte, a condition which adversely effects the cell performance.

Operation of Gould Cell 2-002 (Li-Al/$FeS_2$-$CoS_2$) was terminated after 165 hr of operation because of an electrical short; the cell was examined primarily to determine the source of this short. Cross-sectioning of the cell into successively smaller sections indicated the presence of multiple conductive paths between the negative and positive electrodes. Metallographic examination showed evidence of large particles of carbon cement within the BN fabric separator (the carbon cement was used to bond the graphite cloth retainer to the porous, vitreous carbon current collector). The presence of the carbon cement in the separator is considered the most probable cause of the electric short.

A second $FeS_2$-type cell (2-003) from Gould was operated for 870 hr; operation was terminated when a malfunction in the cell cycler caused overcharge of the cell and a consequent short circuit. The cell was operating quite well until this malfunction occurred. Metallographic and X-ray diffraction analyses* of the positive electrode showed the presence of X and J phases, $Li_2S$, and Fe, which are indicative of an intermediate state of charge. The presence of a significant quantity of metal sulfides within the BN separator has been attributed to agitation that occurs during the electrolyte filling operation. A narrow band of $Li_2S$ was found near the negative electrode/separator interface; no such band had been observed in previous cell examinations.

Eagle-Picher Cell 2B1 (Li-Al/$FeS_2$-$CoS_2$) was operated for 50 hr; operation was terminated because of a fracture of the current collector, as discussed above. This cell had a honeycomb type of current collector in both the negative and positive electrodes. Examination showed that the $ZrO_2$ retainer cloth had been severely cut by the honeycomb structure in many areas. It appears that a protective metal screen will be required to prevent this occurrence in cells with honeycomb current collectors.

---

*X-ray diffraction analyses by B. S. Tani, Analytical Chemistry Laboratory, ANL.

## C. Battery Engineering
(A. A. Chilenskas)

### 1. Systems/Costs Studies
(G. J. Bernstein, A. A. Chilenskas)

Lithium Requirements to the Year 2000. The use of Li-Al/iron sulfide batteries for energy storage on electric utilities and power sources for electric vehicles will create a demand for large quantities of lithium. An attempt has been made to estimate the need for lithium ores and productive capacity in the U.S. for the time period 1985-2000.

The projected lithium requirement for off-peak energy storage batteries is based upon the following estimates for total electrical-energy consumption: $4 \times 10^9$ MW-hr in 1985, $6 \times 10^9$ in 1990, and $10 \times 10^9$ in the year 2000.[3] The fraction of this energy supplied from lithium-aluminum/iron sulfide batteries was estimated to be minimal in 1985, about 1% in 1990, and about 3% in 2000. Based upon these assumptions, the projected energy supplied from battery storage plants in the year 2000 is $3 \times 10^8$ MW-hr. Present-day laboratory test cells, which have a lithium content of 6.5 wt %, have achieved 150 W-hr/kg; about 4% of the lithium is in the electrodes and the remainder is in the LiCl-KCl electrolyte. Assuming 250 charge-discharge cycles per year and the above values, the total amount of lithium in battery systems on utility networks would be about $5 \times 10^8$ kg in the year 2000.

Electric vehicles are expected to be introduced in significant numbers around 1985, with annual production rising to about 2.7 million in the year 2000. Based upon an expected average lifetime of these vehicles of at least 10 years, there would be about 18 million electric vehicles on the road in the year 2000. A typical vehicle would be equipped with a 42 kW-hr lithium-aluminum/iron sulfide battery which would weigh about 350 kg and would be capable of driving the vehicle more than 150 miles per charge. The electric vehicle cells would contain about 7.2 wt % lithium as metal and salt. Thus, each vehicle battery would contain about 15 kg of lithium, to give a total of $2.7 \times 10^8$ kg in vehicle batteries in 2000.

Table II-5 summarizes the total annual requirements for lithium and the total lithium contained in batteries used for energy storage and electric vehicles. The table also shows the effect upon lithium requirements of 90% recycle of the lithium in scrapped batteries. The projected lithium requirement for 2000 represents a substantial fraction of the present estimate of world lithium resources, and is nearly equal to the estimated economically recoverable lithium resources in the U.S.[4] Moreover, the projected market for primary batteries using lithium will add to these requirements. In summary, major expansion of exploration for new sources of lithium and increases in lithium production capacity will be necessary to meet the U.S. goals for petroleum conservation in transportation and electrical power generation.

### 2. Design Studies
(G. J. Bernstein, A. A. Chilenskas)

Conceptual Design of 200 MW-hr Utility Plant. Design studies are being continued to establish cell and battery specifications for use in a utility energy storage system (a conceptual design for a 10 MW-hr battery

Table II-5. Projected U.S. Requirements for Lithium in Lithium-Aluminum/Iron Sulfide Batteries for Utility Energy Storage and Electric Vehicles

| Requirements | 1985 | 1990 | 2000 |
|---|---|---|---|
| Utility Energy, MW-hr | | | |
| Total Consumption | $4 \times 10^9$ | $6 \times 10^9$ | $10 \times 10^9$ |
| Supplied by Batteries | $5 \times 10^5$ | $6 \times 10^7$ | $3 \times 10^8$ |
| Electric Vehicles | | | |
| Annual Production | $8 \times 10^4$ | $7 \times 10^5$ | $2.7 \times 10^6$ |
| Total in Operation | $1.5 \times 10^5$ | $2.1 \times 10^6$ | $1.8 \times 10^7$ |
| Lithium Usage, kg | | | |
| In Utility Batteries | $1 \times 10^6$ | $1 \times 10^8$ | $5.2 \times 10^8$ |
| In Electric Vehicles | $2.3 \times 10^6$ | $3.2 \times 10^7$ | $2.7 \times 10^8$ |
| Total in Use | $3.3 \times 10^6$ | $1.3 \times 10^8$ | $7.9 \times 10^8$ |
| Lithium Production, kg | | | |
| Annual Total for 10-yr Battery Life, No Recycle | $2.2 \times 10^6$ | $3.9 \times 10^7$ | $1.2 \times 10^8$ |
| Annual Total for 10-yr Battery Life, 90% Recycle | $2.2 \times 10^6$ | $3.9 \times 10^7$ | $8.4 \times 10^7$ |
| Cumulative Total, No Recycle | $3.3 \times 10^6$ | $1.3 \times 10^8$ | $9.3 \times 10^8$ |
| Cumulative Total, 90% Recycle | $3.3 \times 10^6$ | $1.3 \times 10^8$ | $8.1 \times 10^8$ |

storage plant was described in ANL-75-1, pp. 124-134). The current effort is directed primarily toward reducing the cost of the storage system through the use of a mass-produced module of 5.5 MW-hr capacity that can be transported by truck. The design of the "truckable" module is based upon a 10-hr discharge rate for load-leveling application and a 5-hr discharge rate for peaking application. An evaluation is being made of the technical and economic effects of increasing the basic cell size from the previous reference size of 31 by 31 cm to 51 by 51 cm.

Table II-6 shows the specifications that have been selected for the reference design of the 200 MW-hr plant. The weight and size limitations shown are the maximum for truck shipment. The modular concept will provide free-standing, self-contained modules with insulation, coolant channels, heaters, cell support structure, bus bars, etc. in an all-weather enclosure ready to be set up at the utility site. Because of the limitation on shipping weight, the cells would be shipped separately and installed at the site.

The preliminary module design is based upon the use of a 51 by 51 by 2.5 cm subcell. This subcell is considerably larger than current experimental prismatic cells (13 by 13 cm) but it is anticipated that improvements in cell design and fabrication methods will make the larger size feasible. A significant advantage would be a reduction in the number of terminal connections required. Figure II-7 shows a sectional view of a subcell. A cell

Table II-6. Specifications for 200 MW-hr Utility Plant

| | |
|---|---|
| Energy Output, MW-hr | 200 |
| Power Output, MW | 20 |
| Duty Cycle, hr | |
| Discharge | 10 |
| Charge | 7 |
| Converter Output (Max.), MW | 6 |
| Maximum Voltage, V | 1000 |
| Maximum Current, A | 10,000 |
| Energy Efficiency, % | 80 |
| Trucking Limitations | |
| Max. Weight, kg | 27,300 |
| Max. Size, m | 12 x 2.5 x 2.75 high |

is made up of 25 subcells connected in parallel. Parallel connection results in an average discharge voltage (at a 10-hr rate) of 1.22 V. The theoretical capacity of each subcell is 2500 A-hr, giving a theoretical cell capacity of 62,500 A-hr. At 80% utilization, the capacity of a cell is 50,000 A-hr. A module contains 90 cells, and six modules are connected in series to form a string. Each module has an energy output of 5500 kW-hr. Studies of packaging of cells into modules and arrangement of cells for interconnection are continuing. Various arrangements of modules and strings are also being evaluated to achieve optimum conditions for handling and cooling. Figure II-8 shows a

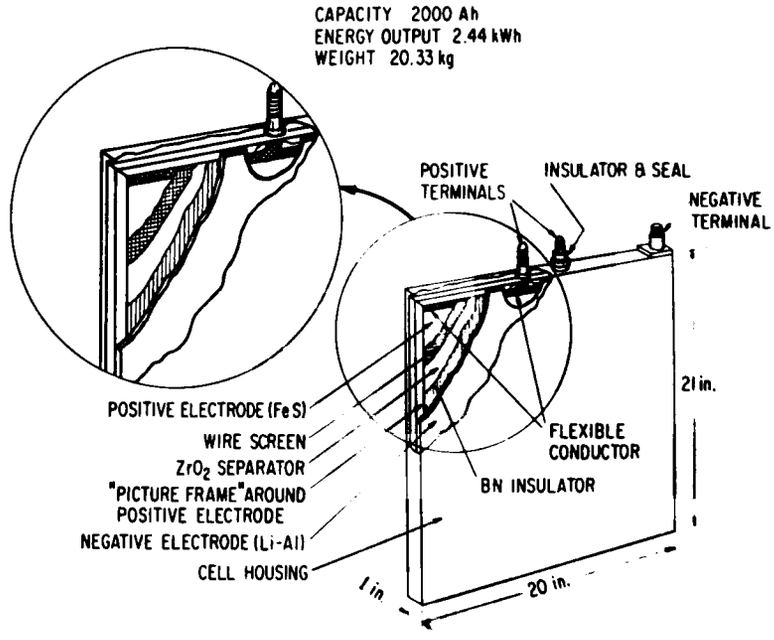


Fig. II-7. Subcell for Truckable Module

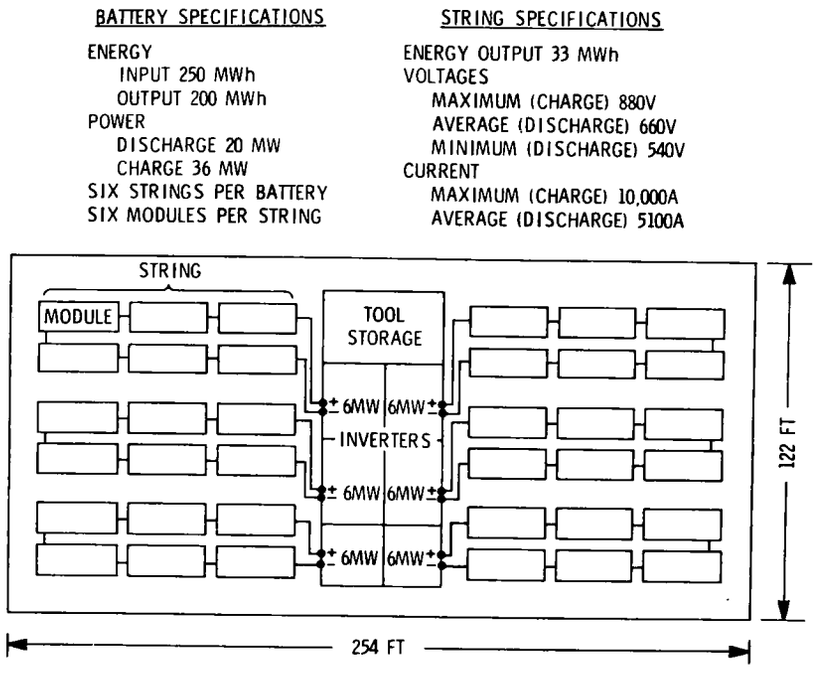


Fig. II-8. 200 MW-hr Utility Energy-Storage Plant

schematic layout of a 200 MW-hr storage plant based upon six modules per string and six strings per battery.

Temperature control of the battery storage system is of critical importance. A desirable cell operating temperature is 400°C (750°F) with a minimum of 360°C (680°F) and a maximum of 425°C (800°F). The maximum temperature is conservative and was selected to avoid any risk of overheating the interior of a cell. Calculations have been made to evaluate the performance of insulation and cooling systems designed to maintain the battery within operable temperature limits under various conditions of operation. The basis for these calculations is the heat developed in the battery during a 10-hr charge or discharge period. It is assumed that 10% of the power generated in the battery will be converted to heat. Accordingly, a module (5500 kW-hr energy output) would generate heat at a 55 kW rate.

The arrangement of cells within a module is shown in Fig. II-9. The cells are mounted in five racks, with each rack containing three layers of six cells each (a cell is made up of 25 subcells). Each module has its own external insulation (protected by a sheet metal enclosure) and air blower system. Sections of the insulation can be removed to permit a six-cell array to be removed and replaced by means of a fork-lift truck equipped with a horizontal ram.

The insulation should be capable of holding the module temperature above 360°C during stand-by conditions for up to 20 hr. The performance of the insulation must be such that a practical balance is made between heat loss during idle conditions and heat loss during peak discharge conditions. Under the latter conditions, when heat generation is high, effective heat loss through the insulation will reduce the requirement for heat removal by the coolant air. It is expected that resistance heaters will be located within the enclosure to provide minimum cell temperature during protracted idle periods or for initial startup.

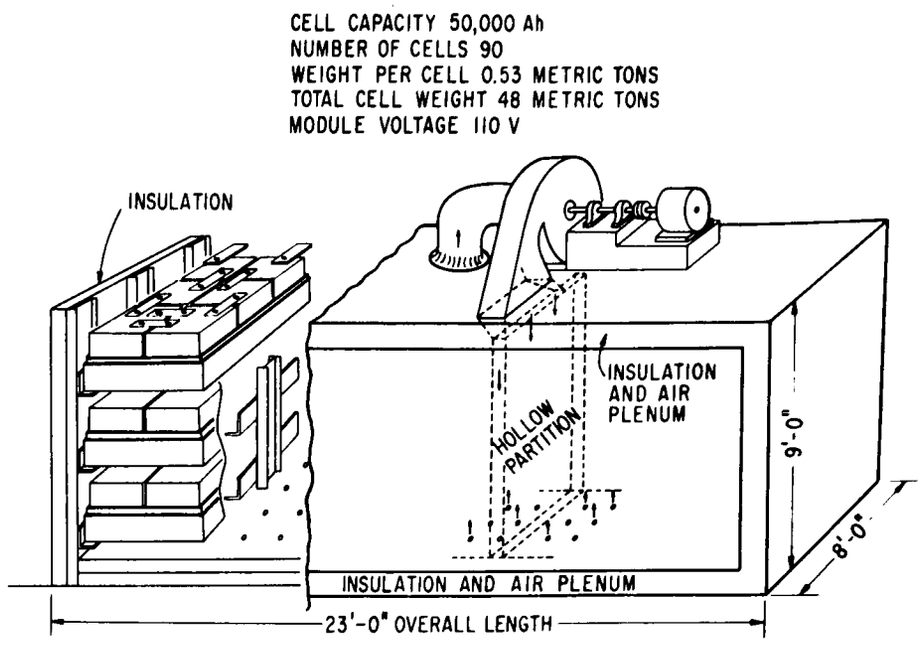


Fig. II-9. Truckable Battery Module (5.5 MW-hr)

Calculated heat conductivity of the cell internals shows that a temperature gradient of about 28°C would exist between the cell internals and surface, which would limit the surface temperature to 400°C. Heat transfer calculations which allow for losses through seams and penetrations show that total heat loss through 10 cm of mineral-wool or aluminum-foil insulation would be about 33 kW. Accordingly, during charging or discharging of the battery at a 10-hr rate, 55 - 33 = 22 kW must be removed by air cooling. Close control of coolant air flow and temperature is required to avoid the risk of excessive cooling at the air-inlet zone and inadequate cooling at the air-outlet zone. One system involves circulation of about 4250 $m^3$/min of air at an average temperature of 383°C or 17°C below the cell wall temperature. An alternative method involves intermittent circulation of a small volume of air, with the direction of flow being reversed at each cycle. Between air flow cycles, the heat generated in the cells would be allowed to heat up the cell.

Further refinements in the insulating and cooling systems are being investigated. In addition, the problem of higher heat generation, such as that of a peaking battery on a 5-hr discharge duty, is under study.

3. Component Testing

a. Multicell Cycler System
(E. C. Berrill, W. W. Lark, F. Hornstra)

In February 1976, a contract was completed with Paraplegics Manufacturing Company to fabricate 26 cell-cycler modules, one of which is shown in Fig. II-10. Included in the above number was a 10-module system housed in a mobile cabinet.

The operating principles of the basic module are illustrated in Fig. II-11. As indicated, the unit consists of an unregulated power supply,

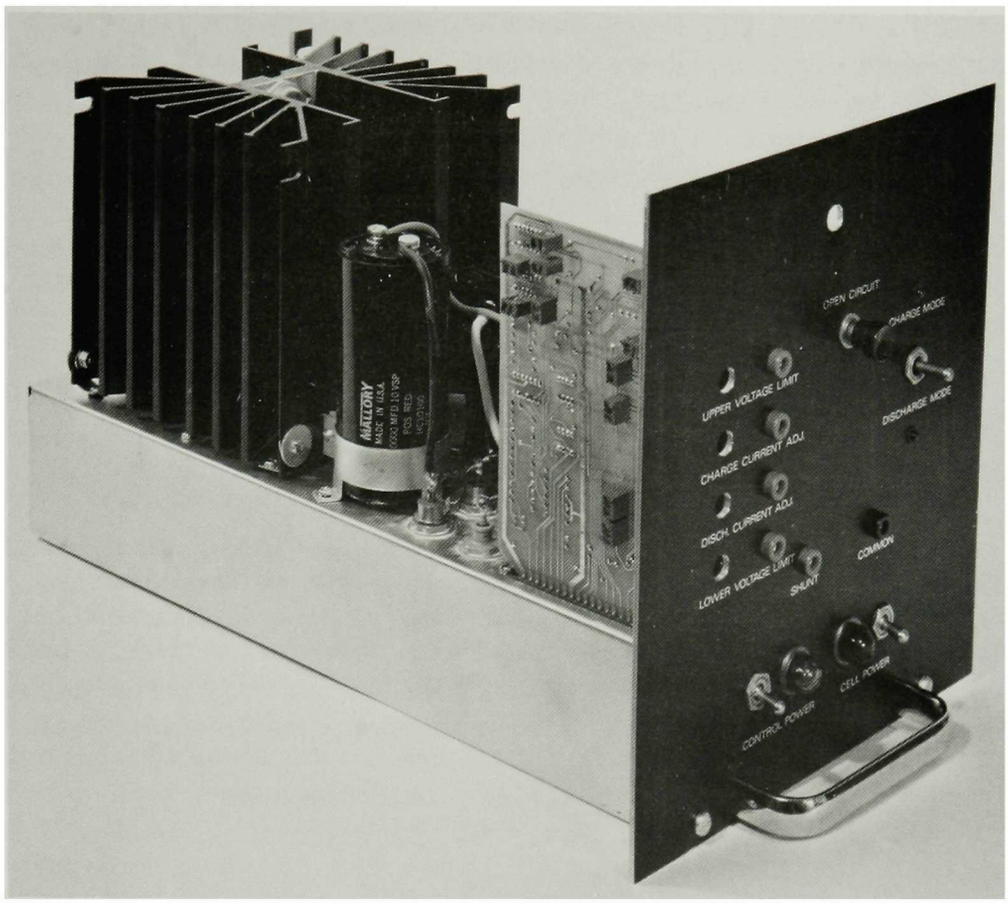


Fig. II-10. Cell-Cycler Module

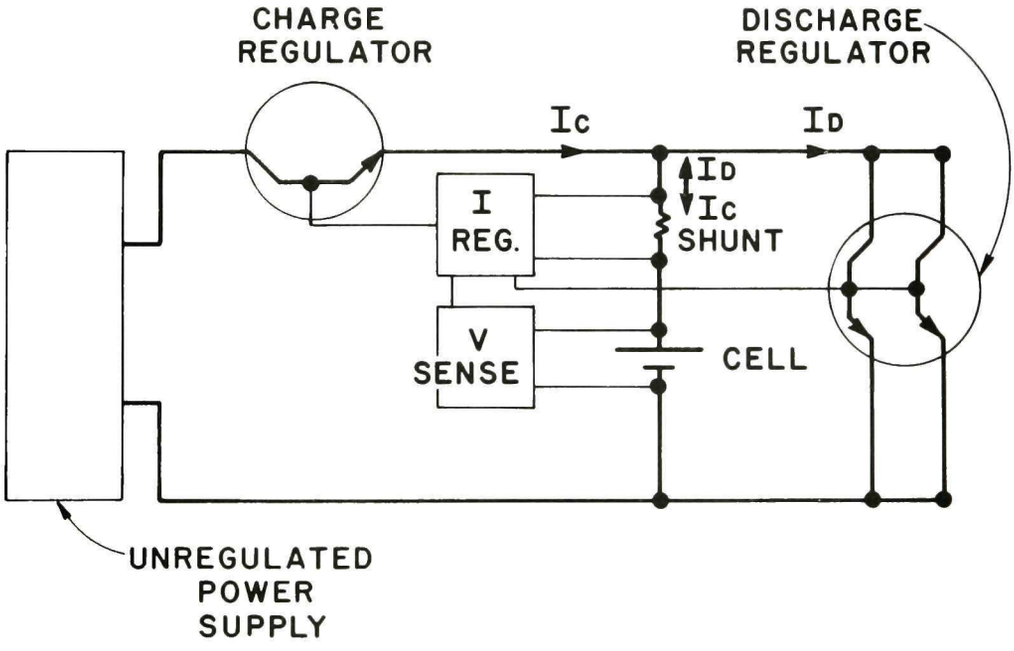


Fig. II-11. Schematic of Cell-Cycler Module

a precision shunt, solid state regulators, and control circuitry. The cell voltage is continuously sensed by a circuit that controls whether the charge or discharge mode is implemented. If the system is started in the charge mode, the charging current ($I_c$) continues, with the discharge regulator turned off, until the selected charge cutoff voltage is reached. The cycler then switches to the discharge mode, in which the charge regulator is turned off and the discharge current ($I_d$) flows through the discharge regulator until the cell reaches the selected discharge cutoff voltage. Then the charge mode is again initiated.

Charge and discharge currents are independently adjustable up to 25 A and are regulated to better than 1%. Charge and discharge cutoff voltages up to 3 V can be selected with a precision of ±0.01 V.

Front panel controls include status-indicating lamps, manual charge/discharge selection, open-circuit test, and buffered meter jacks. A helpful feature incorporated in this design provides the capability to preset each of the variables before turning on the power to the cell; thus, the operating parameters can be previewed without endangering the cell. The modules in lots of five cost $500 each, including parts and labor.

b. Cell Equalization Systems
(E. C. Berrill, J. Cox,* W. W. Lark, C. Russell,** F. Hornstra)

The cells in a Li-Al/$FeS_x$ battery will require periodic equalization of cell voltages to accommodate small differences of coulombic efficiencies among cells. The development of two charge-equalization systems is being pursued. One system is designed specifically for laboratory use and the other is suitable for use on an electric vehicle battery.

The laboratory system that was designed and constructed permits a great deal of flexibility in studying charge equalization parameters and interaction with the main charger on the equalizer system. The complete four-cell laboratory system has a four-cell voltage monitor and four dual-mode, adjustable power supplies.

The control system for cell-voltage monitoring utilizes a differential amplifier connected to each cell. The cell voltage is compared to a preset reference voltage in the high limit (charge cutoff) comparators and simultaneously in the low limit (discharge cutoff) comparators. If any cell voltage is beyond the preset high or low limits, the appropriate comparator generates a signal that causes a latching circuit to be set. The latching circuit acts as a memory unit and, through a front-panel lamp, indicates which cell is beyond which limit. In addition, the comparator signal is used to control the cell equalization system and the existing cell cycler system. Three modes of operation are available, as follows: 1) cells charge and then equalize; 2) cells discharge, charge, and then equalize; and 3) normal cycling continues without an equalization period but within the upper and lower limits (*i.e.*, the cell with the highest terminal voltage determines charge cutoff; the cell with the lowest terminal voltage determines

*Industrial participant from Gulton Industries, Inc.

**Undergraduate student from University of Cincinnati.

discharge cutoff). A panel meter is available for reading each cell voltage and the upper and lower cutoff voltages. Equalization, once initiated, will proceed until stopped manually.

Cell equalization is accomplished by the use of an individual dual-mode power supply connected to each cell. Each power supply is capable of operating in the constant-current or constant-voltage mode, with automatic crossover between modes. In operation, a cell is first charged at a preset constant-current rate, which is controlled by the current regulator in the supply. During this mode, the cell voltage will rise until it reaches a preset charge cutoff level. When this point is reached, a pair of remote voltage-sensing leads signal the power supply, through the voltage regulator circuit, to maintain the cell voltage at the preset limit. The supply now operates in the constant-voltage mode and the cell charging current monotonically decreases to the cell leakage current.

The vehicle equalization system has been designed specifically for use in an electric vehicle, where cost, weight, and simplicity are important considerations. This system was designed under an arrangement with Gulton Industries, in which a member of their staff worked at ANL. A preliminary design analysis was completed; the analysis indicates that a system having all the features desirable for use in an electric vehicle can be built. A cost objective of this design effort was an equalizing system that could be mass produced for about $1 per cell. Gulton has proposed a six-cell prototype equalizer for laboratory tests of the concept. The procurement package for the construction of this prototype is being assembled.

c. Cell and Battery Protective Circuit
(E. C. Berrill, W. W. Lark, F. Hornstra)

A protective circuit was designed and constructed to electrically isolate a battery or a cell from a charge/discharge cycler if a charge or discharge is not terminated at the preset values. As illustrated in Fig. II-12, the protective circuit, which monitors the voltage independently from

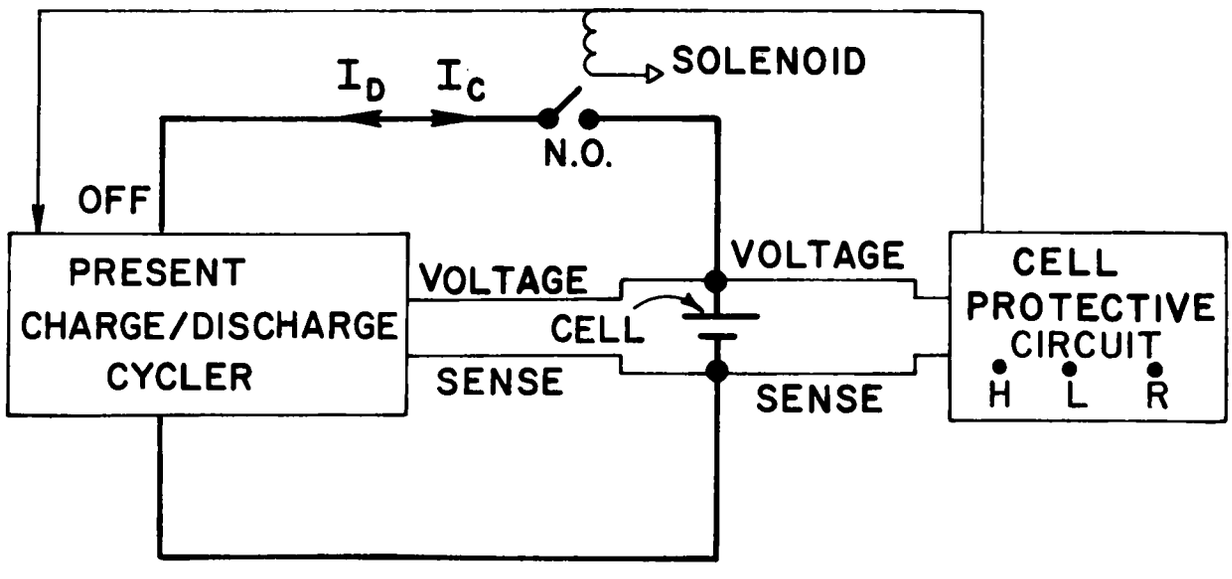


Fig. II-12. Protective Circuit with Present Charge/Discharge Cycler

the cycler, has adjustable upper and lower limits. In practice, these limits are set slightly above and below the respective limits set on the cycler. If the cycler operates beyond these limits, the protective circuit opens a switch between the battery and the cycler, turns off the cycler and turns on a light that signals whether the upper or lower limit was violated. The battery remains isolated from the cycler until the protective circuit is manually reset. In this manner, an independent, redundant voltage monitor precludes a malfunction of the cycler from damaging a battery or cell.

4. Battery Testing
(V. M. Kolba, G. W. Redding, E. C. Berrill)

A small-scale facility (see ANL-76-9, p. 80) for testing cells and batteries has now been completed. This facility permits testing of one thick or two thin cells in each test chamber and monitoring of the current, voltage, and temperature of individual cells while operated in a series or parallel battery arrangement. The first two-cell battery tests were performed with contractor-fabricated cells. These cells were filled with electrolyte using procedures established in the cell fabrication effort, and sealed; they were then removed from the glovebox and subsequently handled in air. The battery is being operated under an argon or helium atmosphere.

Attempts were made to condition and operate two Gould $FeS_2$ cells (2-001 and 2-006), in a series arrangement and later a parallel arrangement, according to established conditioning procedures. These cells had high resistance ($\sim$60 m$\Omega$) and utilization was very poor, but the ampere-hour efficiency was >95%. After completing one test cycle, more electrolyte was added to these cells. This increased the performance somewhat but utilization was still <20%; therefore, testing of these cells was terminated. Two additional $FeS_2$ cells (2-004 and 2-005) having low resistance at room temperature were filled and conditioned individually according to a modified procedure. The utilizations for cells 2-004 and 2-005 at the 10-hr rate were 40 and 60%, respectively, while the ampere-hour efficiencies were 46 and 79%, respectively. After the cells were characterized individually by operation for several test cycles, they were connected in parallel for testing. Initial results indicate an ampere-hour efficiency of 69% and a utilization of 45% at about a 13-hr rate.

Because Cells 2-004 and 2-005 are badly mismatched, they provide an opportunity to examine battery performance under "worst-case" conditions. These cells are being used in the first two-cell series-connected battery with a laboratory-model cell-equalization charger.

D. Industrial Contracts
(R. O. Ivins, V. M. Kolba)

To accelerate the commercial availability of lithium-aluminum/iron sulfide batteries, a rapid and efficient transfer of technology to industry is required. Toward this end, the participation of industrial firms capable of manufacturing materials, components, electrodes, cells and batteries has been sought at an early stage in the development program. Commercial development is being implemented by contracting with industrial firms to (1) develop manufacturing capability for required cell materials, (2) develop manufacturing techniques for electrodes and cells, (3) develop components such as

insulated battery casings, electrical feedthroughs, and charging control systems, and (4) fabricate and test hardware.

1. Cell Fabrication Development
(R. Elliott, R. Malecha)

Development contracts have been made with three industrial firms to develop manufacturing procedures and fabricate test electrodes and cells. The industrial firms are Gould Inc., Eagle-Picher Industries, Inc., and Catalyst Research Corp.

a. Gould Inc.

In January 1976, ANL issued an addendum to the original contract work statement for Gould Inc.; under this addendum, Gould was to develop and fabricate uncharged, carbon-bonded FeS positive electrodes. However, on the basis of work described in Section II.A.2, a decision was made that the carbon-bonded electrode required more developmental work before being incorporated in contractor-produced cells. Meanwhile, successful development and testing of a hot-pressed uncharged positive electrode (Section IV.A) provided an attractive alternative, and the development effort at Gould has been redirected to this type of electrode beginning March 1, 1976. Under this revised addendum, Gould will also conduct operational tests on assembled cells.

b. Eagle-Picher Industries

Eagle-Picher is developing FeS and $FeS_2$ cells which use cold-pressed electrodes having a honeycomb current collector structure. The method of installing the boron nitride separator was revised to incorporate a pre-soaking of the separator in electrolyte (ANL-76-9, p. 17) and thus provide a pre-formed separator. It is anticipated that this method will provide greater insurance against internal shorting. Two prototype FeS cells and two $FeS_2$ cells were delivered to ANL for testing and evaluation. After successful testing of an FeS cell at ANL, Eagle-Picher was authorized to complete the assembly of all FeS cells. The $FeS_2$ prototype cells were also evaluated and found to have a common failure mode (see Section II.A.1). The failures occurred at the point where the molybdenum current collector sheet is attached to the molybdenum current lead. Further development of joint attachment methods was initiated by both ANL and Eagle-Picher. Based on these efforts, ANL has specifically recommended that this attachment be made with a single rivet followed by brazing for the $FeS_2$ electrodes, and cells fabricated by this technique are scheduled for delivery in April 1976.

c. Catalyst Research Corp.

At Catalyst Research, all equipment required to carry out the contract work has been installed and is now operational. A hood, which has been installed in a dry room having an atmosphere containing 300 ppm $H_2O$, is capable of maintaining a moisture level of less than 10 ppm at the work surface. Development of casting methods for producing the negative electrodes has proved to be more difficult than anticipated. The process requires the infiltration of the Retimet structure with Li-Al alloy. The design of hardware for induction casting of the Li-Al and for rapid cool-down of the electrode is proceeding. Cycling equipment for cell testing has been completed.

The furnaces required for testing cells outside of a glovebox have been designed and tested.

2. Component Development

a. Separator Development
(J. Battles)

The development of improved separators is being pursued under contracts with Carborundum Co., the University of Florida, Zircar Products, Inc., and soon a contract will be made with Fiber Materials, Inc.

Carborundum Co. Significant progress has been made in the development of a low-cost, porous electrode separator. Development efforts under the Carborundum contract have been concentrated on improving the fabrication process that uses a combination of BN and $B_2O_3$ fibers. In this process, the BN fibers are bonded during the conversion of the $B_2O_3$ fibers to BN. Cell tests of samples supplied by Carborundum showed that the fiber bonds were sufficiently strong to retain the paper structure after ∿350 hr of operation. Carborundum is also pursuing a different approach in which papers are fabricated from $B_2O_3$ fibers which are then converted to BN. The initial tests have been encouraging and the simplicity of the process should yield a cost reduction. Effort is being placed on improving fiber distribution, pore size control, porosity and thickness.

University of Florida. The major emphasis of the separator development program at the University of Florida is on the fabrication of composite-type separators using various combinations of fibers and ceramic powders. A variety of paper samples using various combinations and concentrations of ceramic fibers and powders (BN, $LiAlO_2$, $Y_2O_3$, MgO) have been supplied to ANL. Asbestos fibers (5-20%) were used as binders in these samples. The mechanical and physical properties are being determined. Cell tests are being conducted on an $Y_2O_3$-10% asbestos paper sample. The cell has operated more than 500 hr, and performance continues to be very satisfactory. This is the best result obtained to date with a paper separator.

Zircar Products, Inc. At our request, Zircar prepared fibers and felts of $Y_2O_3$ electrode separators. The quoted costs for the $Y_2O_3$ felts are \$112/ft$^2$ and \$36/ft$^2$ for quantities of 100 and 1000 ft$^2$, respectively. For large quantities such as $5 \times 10^6$ ft$^2$, the estimated cost is about \$3/ft$^2$, a value that approaches the cost goals for separators. Preparations are now under way for in-cell testing and mechanical and physical characterization of these felts.

Fiber Materials, Inc. A development contract for fabricating BN paper separators is to be initiated with Fiber Materials, Inc. to provide a second source of BN fibers. Emphasis in this development program will be on the evaluation of four different paper-making concepts not covered in other contracts. These concepts will be discussed in more detail in a later report.

b. Feedthrough Development
(K. M. Myles)

The design and development of electrical insulators and compact, low-cost electrical feedthroughs is being undertaken by contracts with National Beryllia, Ceramaseal, ILC Technology, 3M Company, and Coors Porcelain. The status of the expanded effort on development of mechanical and brazed type feedthroughs is summarized below.

National Beryllia. This effort involves the development and fabrication of BeO insulators to replace the BN lower insulators in the modified Conax feedthrough and the ANL redesigned feedthroughs. The stronger BeO will allow further tightening of the feedthrough, with an expected improvement in leak-tightness. Delivery of the parts is expected in mid-March 1976.

Ceramaseal. A ram-type feedthrough is being developed in this contract effort, and six prototype units have been received. Five of these have a copper sealant between the metal and ceramic, and one has a gold sealant. These units will be evaluated in a testing program at ANL. Preparation of a proposal to investigate methods of reducing the size of the ram-type feedthrough is being discussed with the contractor.

ILC Technology. A number of niobium-base brazed feedthroughs having BeO insulators have been fabricated and delivered. Testing and evaluation is presently under way (see Section II.B). Future efforts with this type of feedthrough await results of these tests.

3M Company. Prototype BeO feedthroughs have been fabricated and delivered. In these units, the conventional metallization brazes were overplated with a protective layer of nickel or gold. These feedthroughs are also under test and evaluation, but no further development effort is contemplated.

Coors Porcelain. This is a new contractual effort covering development of a method to permit $Y_2O_3$ parts to be brazed using a non-metallic-type braze.

c. Electrolyte and Active Material Sources
(Z. Tomczuk)

Industrial sources of active materials and electrolyte are needed for larger volume production of cells. Efforts during this report period have been directed toward improving the quality and reducing the cost of these materials. The source and purity of electrolyte and some of the active materials used in developmental and commercial cells are given in Table II-7. Discussions are continuing with Lithcoa toward upgrading the quality of the LiCl-KCl electrolyte which they supply.

Particular emphasis has been placed on low-cost methods for preparation of $Li_2S$, because this is the key material necessary for producing Li-Al/$FeS_x$ cells in the uncharged state. Meetings were held with representatives of Foote Mineral, Eagle-Picher, and Lithcoa to discuss alternative, lower-cost methods of producing $Li_2S$. Preliminary cost analyses of possible

Table II-7. Source and Purity of Available Positive-Electrode Materials and Electrolyte

| Material | Source | Stated Purity, % |
|---|---|---|
| CoS | Great Western Inorganic | 99 |
| $CoS_2$ | Cerac/Pure Inc. | 99 |
| $Cu_2S$ | Great Western Inorganic | 99 |
| $Li_2S$ | Foote Mineral | 97 |
| $Li_2S$ | Eagle-Picher | a |
| LiCl-KCl | Lithcoa | >99.8[b] |

[a] Samples of $Li_2S$ have been obtained from Eagle-Picher and are being used in operating cells. Analyses performed on this material, to date, are presented in Section III.B.

[b] Major impurity is $BaCl_2$; $OH^-$, $O^{2-}$, and $CO_3^{2-}$ impurities total <500 ppm.

methods for producing $Li_2S$ indicate that the method utilizing the high-temperature reaction

$$Li_2CO_3 + H_2S \xrightarrow[\Delta]{700\text{-}900^\circ C} Li_2S + H_2O + CO_2$$

should yield a product costing less than $10/lb if production is scaled up to the pilot plant stage. This reaction scheme is particularly attractive because (1) the starting materials, $Li_2CO_3$ and $H_2S$, are available in high purity and at low cost; (2) the product material is crystalline, not amorphous, and thus its reactivity with moisture is decreased; and (3) the resulting product material is of high purity (>97%).

d. Cell and Battery Charging
(F. Hornstra)

This effort is directed toward the development and fabrication of cell-equalization and battery-charging equipment. An industrial-participant contract with Gulton Industries, Inc., ending in February 1976, had as its objective the design of a battery-cell equalization system suitable for use on electric vehicle batteries. The design constraints included low cost (~$1 per cell for mass-produced units), light weight, simplicity, and reliability. The industrial participant thoroughly analyzed the cell characteristics and proposed a system which appears to be satisfactory. A six-cell demonstration prototype for laboratory use will be constructed when funding becomes available. Subsequent phases of this effort should include an investigation of the interaction of the main charger with the cell equalization unit and subsequently the construction and testing of a complete vehicle battery charging system.

## REFERENCES

1. R. C. Anderson and J. Barker, "A Unique Optical Ceramic," *Optical Spectra,* p. 57, (January 1967).

2. R. M. Gruver, W. A. Sotter, and H. P. Kirchner, "Variations of Fracture Stress with Flaw Character in 96% $Al_2O_3$," Ceramic Bull. *55*(2), 198 (1976).

3. *Electric Utility Industry R&D Goals Through the Year 2000,* Electric Research Council Publication No. 1-71, Appendix F.

4. J. D. Vine, U.S. Dept. of Interior, Geological Survey, personal communication, 1975.

# III. CELL CHEMISTRY
(R. K. Steunenberg)

The objectives of the cell chemistry studies are (1) to investigate specific chemical and electrochemical problems that arise in the cell and battery development work, (2) to conduct studies that are expected to lead to improvements in the electrode and cell designs, and (3) to provide a basic understanding of the processes that occur within the cells.

## A. Evaluation of Fe-Mo-Ni Foametal* Current Collector
(Z. Tomczuk, A. E. Martin)

Because of the cost and the fabrication problems associated with molybdenum current collectors for $FeS_2$ electrodes, alternative current-collector materials and structures are being evaluated in a cooperative effort with the Materials Group. A Li-Al/$FeS_2$ cell was operated with a porous Fe-Mo-Ni Foametal current collector in the $FeS_2$ electrode. This material was chosen because the oxidation potential of a similar alloy had been found to be higher (2.3 V) than the voltage normally used to charge Li-Al/$FeS_2$ cells.

The electrical performance of the cell was excellent. The coulombic efficiency was greater than 95%, and the $FeS_2$ utilization was over 80% of the theoretical value after the initial break-in cycles. The utilization was unexpectedly high in view of the fact that the operating temperature was lower than usual (406 *vs.* 430°C), and the charge cutoff voltage lower than normal (2.00 *vs.* 2.15 V). The current density was kept low ($\sim$18 mA/cm$^2$) to evaluate possible side reactions.

Although the overall electrical performance was excellent, the coulombic efficiency declined slightly with cycling time and the shapes of the voltage-*vs.*-capacity curves changed somewhat. The length of the upper voltage plateau during discharge decreased slightly, that of the second plateau increased, and a short third plateau was observed at about 1.15 V *vs.* Li-Al. The length of the third plateau increased slightly with cycling time but after $\sim$430 hr of cell operation, it represented less than 5% of the discharge capacity.

A preliminary post-test examination of the Foametal current collector revealed that some attack had occurred; this result was not unexpected in view of the changes that had occurred in the shapes of the discharge curves. The extent of attack was small, however, and it is possible that the use of a slightly higher discharge cutoff voltage (*e.g.*, $\sim$1.15 V instead of $\sim$1.0 V) would result in even less attack.

The results of the above test indicate that a lower operating temperature can be used without a loss of cell performance if a suitable continuous metallic structure is used as the current collector in the positive electrode. This material, however, must meet the requirements of (1) a high oxidation potential (>2.15 V *vs.* Li-Al), (2) chemical inertness toward $FeS_2$, and (3) ready availability at an acceptable cost.

---

*Composition in wt %: Ni-5Fe-26Mo; produced by Foametal, Inc.

## B. Evaluation of Lithium Sulfide
(Z. Tomczuk, A. E. Martin)

Because of the increased interest in Li-Al/$FeS_x$ cells fabricated in the uncharged state, the availability of high-quality $Li_2S$ has assumed greater importance. Most cells of this type that have been tested to date have utilized $Li_2S$ produced in limited quantities by the Foote Mineral Co. Consideration is now being given to other methods of preparation that may produce less expensive $Li_2S$ having physical properties that are more suitable for use in cells.

At our suggestion, Eagle-Picher Industries, Inc. has developed a process for producing $Li_2S$ by the reaction of $H_2S$ with $Li_2CO_3$ in a graphite container at temperatures of 700-800°C. The results of various tests that were conducted on two lots of $Li_2S$ prepared by this method are reported in Table III-1.* The yellow color of the Lot 9 material is attributed to a minor amount of an unidentified impurity. The effect of this impurity on cell performance has not yet been determined. As indicated in Section IV of this report, the purer material (Lot 8) has been used successfully in Cell R-8.

*X-ray diffraction by B. S. Tani, and sulfur and lithium analyses by W. E. Streets, Analytical Chemistry Laboratory, ANL.

Table III-1. Characteristics of $Li_2S$ Prepared by the Reaction of $H_2S$ with $Li_2CO_3$[a]

| | Lot 8 | Lot 9 |
|---|---|---|
| Chemical Analysis (Eagle-Picher) | | |
| Lithium, wt % | 28.9 | 29.2 |
| Sulfur, wt % | | |
| CdS Precipitation Method | 69.4 | 66.0 |
| Iodine Titration Method | 71.7 | 69.1 |
| Li:S Atomic Ratio | 1.92 | 2.04 |
| | 1.86 | 1.95 |
| Chemical Analysis (ANL) | | |
| Lithium, wt % | 29.45 | 29.75 |
| Sulfur, wt % | 67.26 | 64.88 |
| Li:S Atomic Ratio | 2.023 | 2.119 |
| General Appearance | white granules | yellow granules |
| Metallographic Characteristics | well crystallized $Li_2S$ | well crystallized $Li_2S$ + minor unidentified gray phase |
| X-Ray Diffraction | $Li_2S$ only | $Li_2S$ + one additional line, possibly $Li_2C_2$ |
| In-Cell Tests | R-8 | not yet tested |

[a]Prepared by Eagle-Picher Industries, Inc.

## C. Electrolyte Studies
(J. P. Ackerman, J. W. Sim)

Work has continued on the identification of low-melting molten-salt electrolytes with a high concentration of lithium ions. The ternary system, LiF-LiCl-LiBr (22-31-47 mol %), has performed well as an electrolyte in cell tests, but it has a rather high density (2.19 g/cm$^3$ at 500°C) and is relatively expensive because of its high LiBr content. A redetermination of the liquidus temperature has indicated a value of 445°C, rather than the value reported in the literature (~430°C).[1]

The effect of adding small amounts (10 at. %) of potassium ion to various LiF-LiCl-LiBr compositions was investigated with the objective of finding a low-density, inexpensive mixture with a low liquidus temperature. Figure III-1 shows projections of liquidus isotherms on the LiF-LiCl-LiBr phase diagram.[1] Compositions along lines LiF-A, LiF-B, and LiF-C with the cation composition altered to 90 at. % $Li^+$-10 at. % $K^+$ were investigated by thermal analysis and visual observation, using calibrated thermocouples traceable to the National Bureau of Standards.

Figure III-2 shows the liquidus temperature as a function of fluoride ion content along lines LiF-A, LiF-B, and LiF-C, from Fig. III-1. It is clear that additions of small amounts of potassium ion to the LiF-LiCl-LiBr system decrease the liquidus temperatures significantly in regions of low fluoride ion content. However, such additions also tend to enlarge the LiF phase field, *i.e.*, the lowest melting compositions are lower in fluoride ion content than those in the LiF-LiCl-LiBr system. The liquidus temperatures are highly sensitive to small changes in composition, which is an undesirable feature for an electrolyte. Since substantial concentrations of bromide ion are still required to attain low liquidus temperatures, there are no significant benefits in terms of decreasing the density and cost.

Brief consideration was given to the addition of sodium, rather than potassium ion, to the LiF-LiCl-LiBr system. A review of related phase diagram data in the literature, however, indicated that the liquidus temperatures would be expected to increase. Consequently, no further studies of this system are planned.

## D. Wetting Characteristics of LiCl-KCl Electrolyte
(J. G. Eberhart)

The wettability of separator and particle-retainer materials by the electrolyte is an important factor in cell design considerations. The molten LiCl-KCl electrolyte must wet and penetrate these fabrics, papers, or screens to permit easy passage of lithium ions through these materials as the cell is charged and discharged. Two types of measurements are being made to characterize wettability: (1) the contact angle of the molten salt on solid surfaces of the materials of interest, and (2) the penetrability of fabrics, papers or screens made of these materials by the molten salt. Further tests of both properties were performed with Type 304 stainless steel solid surfaces and 325-mesh screen and with boron nitride paper.

The results of these and earlier tests are summarized in Table III-2. The advancing and receding contact angles, $\theta_A$ and $\theta_R$, show a large hysteresis,

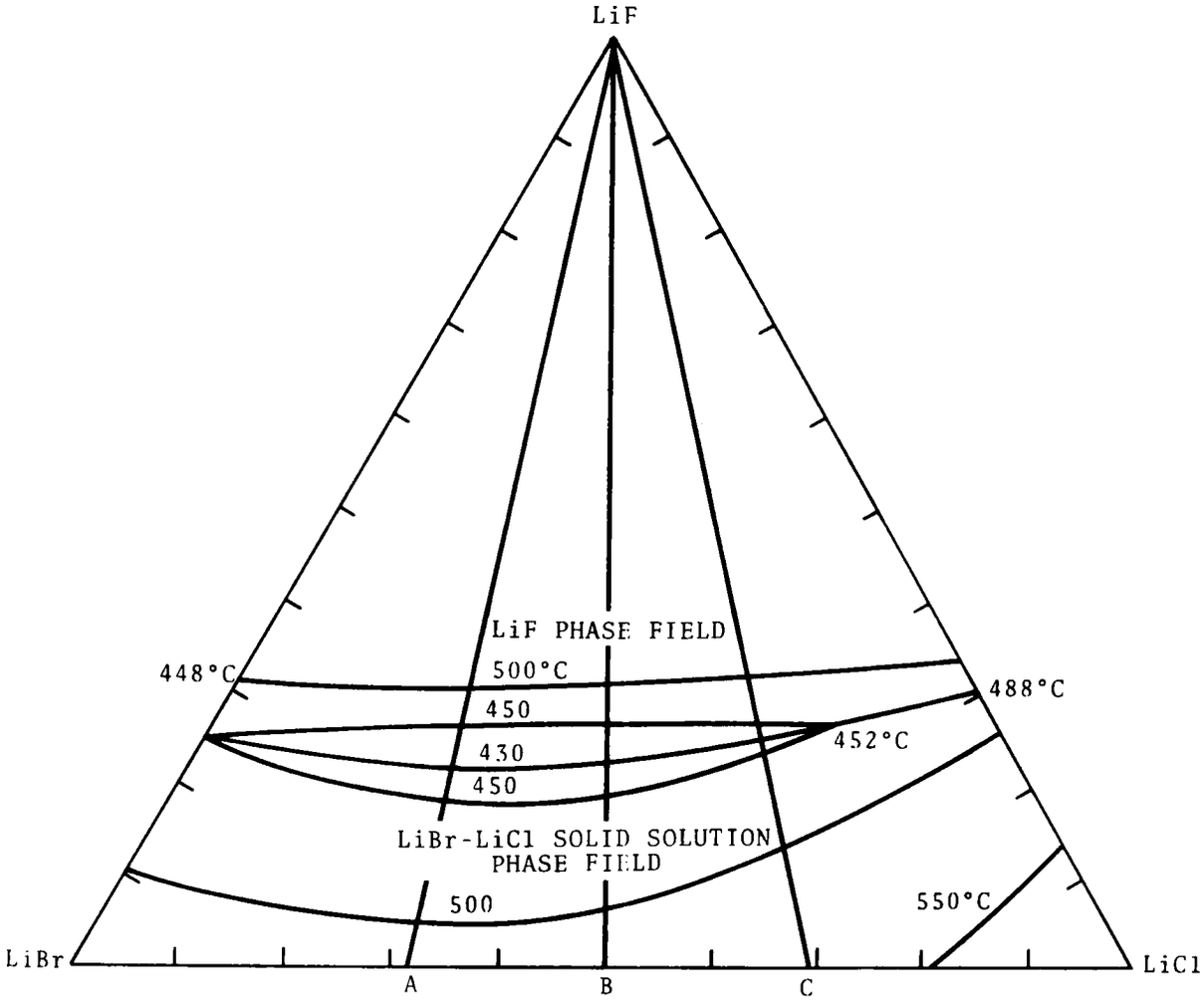


Fig. III-1. LiF-LiCl-LiBr Phase Diagram

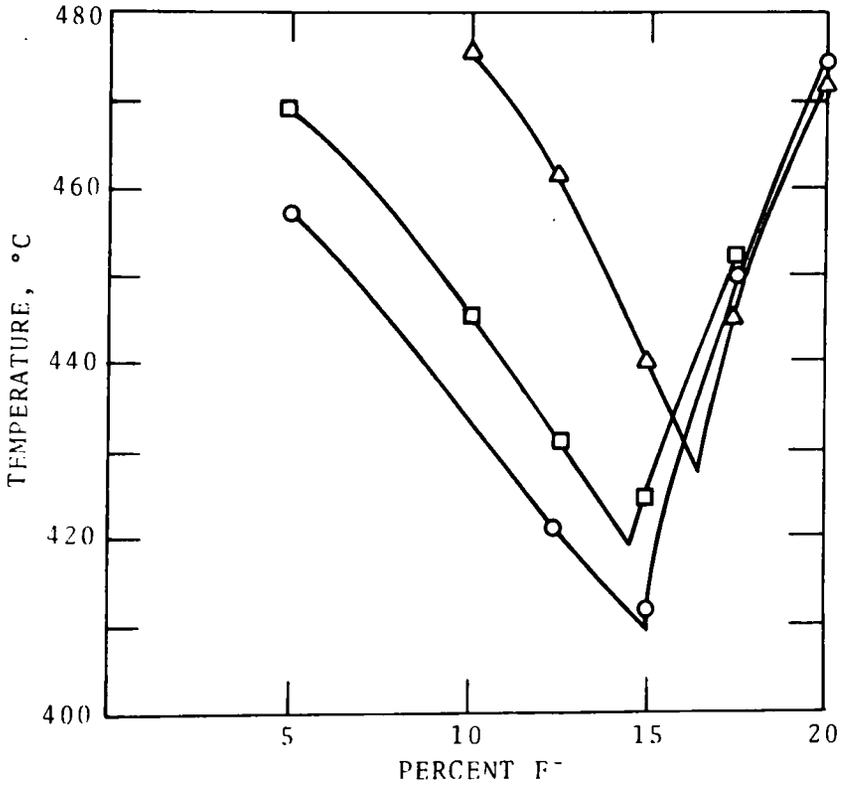


Fig. III-2.

Liquidus Temperature *vs.* $F^-$ Content for 90% $Li^+$-10% $K^+$

○ Line LiF-A (Br/Cl, ∿2.16)

□ Line LiF-B (Br/Cl, ∿1.1)

△ Line LiF-C (Br/Cl, ∿0.45)

Table III-2. Wetting Properties of Separator and Particle-Retainer Materials by Molten Salt[a]

| Material | Solid Surface Contact Angles, deg | | Penetration of Screen or Fabric by Salt |
|---|---|---|---|
| | $\theta_A$ | $\theta_R$ | |
| 304 SS | 93 | 10 | easy |
| $ZrO_2$ | 105 | 45 | easy |
| C | 117 | 55 | difficult |
| BN | 138 | 54 | difficult |

[a]Contact angles were measured at 375°C; penetrabilities were determined at 400°C.

$\theta_A - \theta_R$, on all of these solids. The values of the advancing contact angles indicate that stainless steel and zirconia are more wettable than carbon or boron nitride. These results are borne out by the penetrability tests, which show that stainless steel screen and zirconia fabric are readily penetrated by the molten salt, whereas carbon fabric, boron nitride fabric, and boron nitride paper are difficult to penetrate. The materials that are easily penetrated are wet spontaneously when immersed in the molten salt in a helium atmosphere. The materials that are not penetrated easily are not wet spontaneously under the above conditions. They can be wet, however, by evacuating the system and repressurizing with helium while molten salt is in contact with both surfaces.

Since contact-angle hysteresis is a key factor in the wettability of separator and retainer materials, it is important to understand the cause of the hysteresis. Current theories relate hysteresis effects primarily to roughness and chemical heterogeneity of the surface. It is also possible that exposure of a metallic or ceramic surface to molten salt may alter its surface composition. For example, the molten salt may dissolve a surface oxide layer, causing the advancing molten salt to be in contact with an oxide surface while the receding salt is in contact with a metallic surface. To test this possibility, $\theta_A$ was measured with the molten salt on a zirconium metal surface as a function of time. In Fig. III-3 these results are compared with constant values of $\theta_A$ and $\theta_R$ on a zirconia surface. The initial value of $\theta_A$ for zirconium was in close agreement with that for zirconia, which suggests that the metal surface was covered initially with an oxide layer, as expected. With passing time the drop assumed increasingly lower values of $\theta_A$ with a corresponding increase in liquid-solid contact area. The final value of $\theta_A$ for zirconium was in close agreement with $\theta_R$ for zirconia. These results support the hypothesis of a hysteresis effect caused by a chemical interaction between the oxide surface layer and the molten salt.

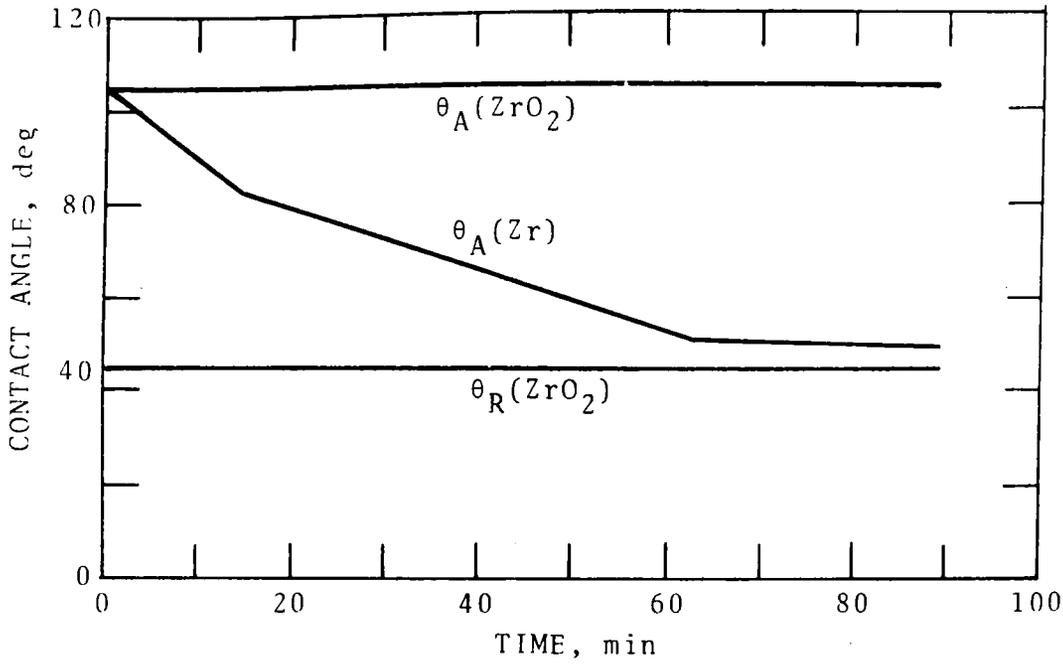


Fig. III-3. Contact Angles of Molten Salt on Zirconia and Zirconium

## REFERENCE

1. A. G. Bergman and A. S. Arabadzhan, Zhur. Neorg. Khim. *8*, 1228 (1963).

# IV. ADVANCED CELL ENGINEERING
(W. J. Walsh)

The effort in this part of the program is directed primarily toward the development and testing of Li-Al/$FeS_x$ cells having improved performance and/or lower cost. The work, which is presently concentrated on the development of advanced electrodes and cell configurations, complements the effort on commercial development, so that any technical advances can be incorporated as quickly as possible into the cells that are being fabricated by industrial firms. Development work is presently centered on Li-Al/$FeS_x$ cells that are assembled in the uncharged state. In a cell of this type, the positive electrode is initially prepared from a mixture of iron powder, $Li_2S$, and electrolyte, and the negative electrode consists of a porous aluminum plaque. Upon charging, the lithium in the positive electrode is electrochemically transferred to the negative electrode, where it reacts to form a lithium-aluminum alloy; concurrently, FeS (or $FeS_2$, depending on the Fe/$Li_2S$ ratio) is formed in the positive electrode.

Engineering work on alternative secondary cell systems, which is just beginning, is reported in Section V below.

## A. Uncharged Li-Al/FeS Cells
(H. Shimotake, L. G. Bartholme)

The development of uncharged Li-Al/FeS cells[1] has solved several major problems that had been previously encountered with FeS-type cells, namely, excessive swelling of the positive electrode, low utilization of the active material in the positive electrode, and gassing from both electrodes. In the present fabrication procedure, the use of sintered $Li_2S$ (see ANL-76-9, p. 55) results in a pressed compact with improved physical characteristics.

A potential disadvantage of this type cell is that the capacity may be limited by the negative electrode, unless extra lithium capacity (Li/S, >2) can be provided. Results to date indicate that after the first formation cycles, between 10 and 20% of the lithium remains in the negative electrode and does not contribute to the cell capacity in subsequent discharges under normal operating conditions. To overcome this problem, methods of providing additional lithium have been sought, and several have been tested. Cell R-9 was assembled with an excess of $Li_2S$ over that calculated for the theoretical capacity of the cell. Although Cell R-9 showed excellent performance, the addition of extra $Li_2S$ may be undesirable because of corrosion problems related to the free sulfur that remains in the positive electrode.

Lithium carbide ($Li_2C_2$) has also been investigated as a source of additional lithium. The addition of $Li_2C_2$ to the positive electrode offers a promising means of providing a Li/S ratio >2. (Studies of the behavior of $Li_2C_2$ in an electrochemical cell are described in Section IV.C.1, below.) The effect of $Li_2C_2$ in a Li-Al/FeS cell was investigated in Cell R-10, a fairly compact, uncharged cell that was similar to Cell R-7 (see ANL-76-9, p. 14), except for the $Li_2C_2$ addition. Figure IV-1 shows the first two charge (or formation) cycles of Cell R-10. The voltage plateau at about 0.78 V (*vs.* Li-Al) observed during charge Cycle 1 is attributed to the electro-

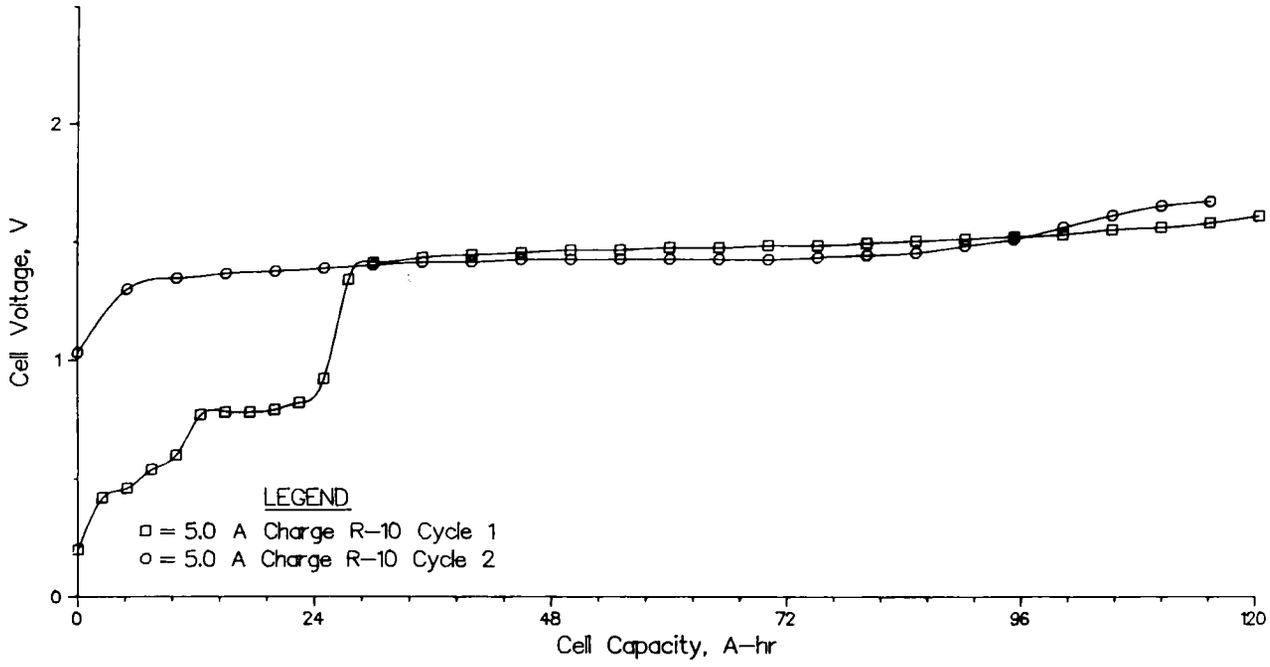


Fig. IV-1. Charge Cycles 1 and 2 for Cell R-10 (theoretical capacity, 150 A-hr)

chemical dissociation of $Li_2C_2$; thus, the re-formation of $Li_2C_2$ can be avoided if the cell voltage is maintained above ∿0.78 V.

The addition of the carbide clearly improved the achievable capacity of the cell. Figure IV-2, which compares the performance of Cell R-7 and Cell R-10 for the same discharge rate, demonstrates that Cell R-10 achieved a capacity about 15% greater than that of Cell R-7. The overall performance of Cell R-10 at different discharge rates is presented in Fig. IV-3. The cell

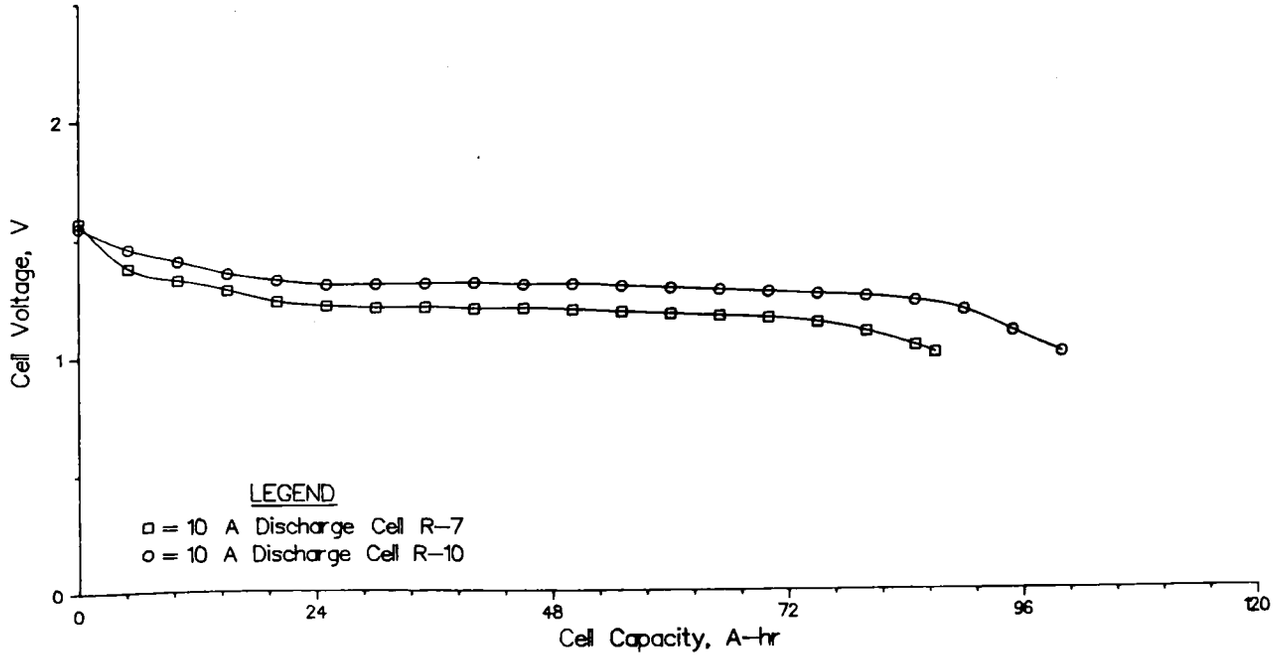


Fig. IV-2. Comparison of Performance of Cells R-7 and R-10

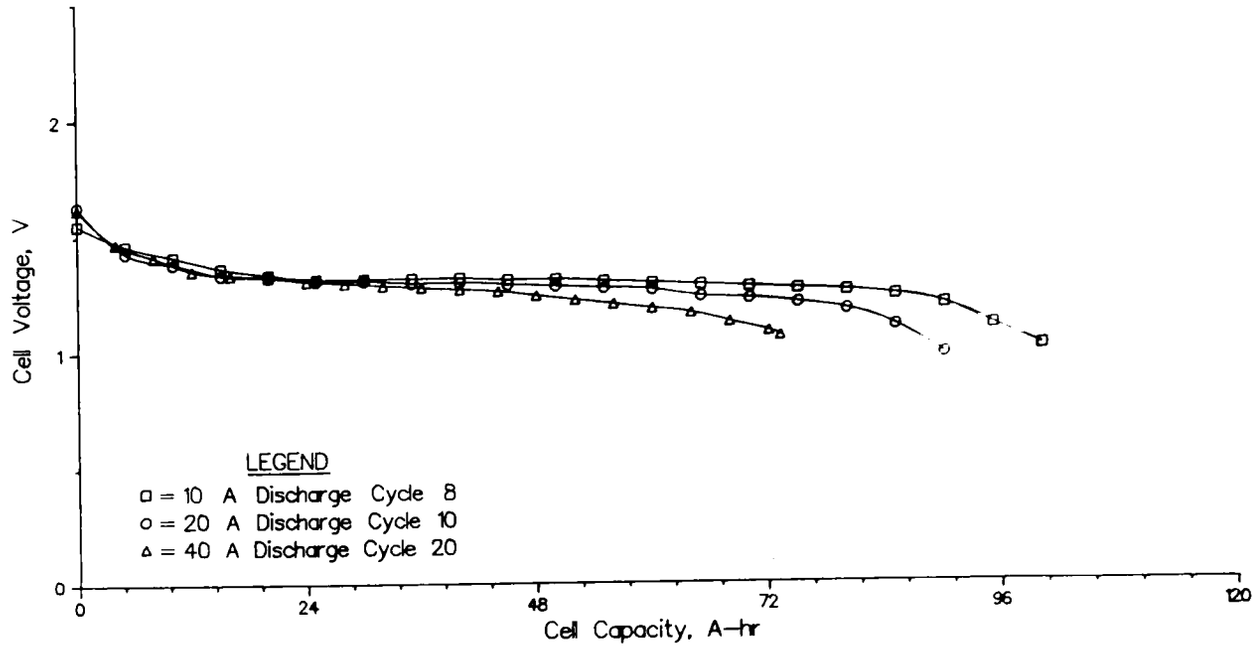


Fig. IV-3. Capacity of Cell R-10 as a Function of Discharge Rate

also demonstrated a capability to discharge up to 50% of theoretical capacity in 2 hr (40-A discharge) with a cutoff voltage of 1 V. An estimated specific energy of about 100 W-hr/kg has been obtained at the 10-hr rate. This is an unusually high specific energy for a Li-Al/FeS cell. The combination of assembling the cell in the uncharged state and adding $Li_2C_2$ to the positive electrode has resulted in a major advance in the performance of Li-Al/FeS cells.

The ampere-hour efficiency of Cell R-10 has been somewhat lower than previous cells, namely, ∿85%. The causes of this low value are being investigated.

## B. Uncharged Li-Al/$FeS_2$ Cells

(J. D. Arntzen, W. J. Walsh)

Cells R-2 and R-3, described in the preceding report (ANL-76-9, p.15), demonstrated the improved performance of uncharged, hot-pressed $FeS_2$-type electrodes. Early attempts to hot press uncharged $FeS_2$ electrodes using sintered $Li_2S$ were unsuccessful. When the $Li_2S$, Fe, $CoS_2$, and LiCl-KCl were pressed at 64,000 kg force (13.7-cm square die) and 400°C the electrode plate was unsatisfactory. In every case the product was crumbly, brittle and did not have the strength and integrity required. The procedure developed for producing an improved uncharged $FeS_2$ electrode plate utilizes a high-temperature treatment in which the electrode constituents are ground to -45 mesh and blended; the mixture is then heated to a temperature of 750 to 800°C for about 10 min, cooled, ground roughly to allow uniform distribution in the pressing die, and hot-pressed at 11,000 kg and 400°C. The electrode plates produced in this manner are uniform and possess satisfactory strength.

In Cell R-8, two uncharged $FeS_2$-type electrode plates prepared by the new technique were assembled to form a positive electrode with a 0.13-mm-thick molybdenum current collector in the center. Aluminum demister-wire structures with iron screen current collectors comprised the facing negative electrodes. Cell R-8 is approximately 2 cm thick and has a theoretical capacity of 90 A-hr. The sintered $Li_2S$ used for this cell was prepared by Eagle-Picher Industries, Inc.; one of the objectives of this cell test is to evaluate this material for use in uncharged cells. (The Eagle-Picher $Li_2S$ is discussed further in Section III. B, above.)

Cell R-8, like previous uncharged cells, showed very little gas evolution. The cell has been operated for 79 cycles and 887 hr as of this writing. In preliminary peak power testing, a specific power of ∿100 W/kg was sustained for 10 sec. The utilization is about 85% of theoretical and the ampere-hour efficiency is 98%. It is concluded that the new $FeS_2$ electrode pressing technique is satisfactory, and that the Eagle-Picher $Li_2S$ may be of acceptable quality. The 85% utilization is unusually high for an uncharged cell without supplemental lithium capacity.

## C. Supporting Studies

### 1. Lithium Carbide Studies
(D. R. Vissers, K. E. Anderson)

As discussed in Section IV. A, above, one of the methods being considered for providing a Li/S ratio greater than two is the addition of lithium carbide ($Li_2C_2$) to the positive electrode. During the first charge cycle, the $Li_2C_2$ would electrochemically decompose, lithium would be transferred to the positive electrode, and a fine graphite powder would remain in the positive electrode. In earlier studies (ANL-75-1, p. 117), the free energy of formation of $Li_2C_2$ was estimated to be -23.1 kcal/mol and the emf (*vs.* Li), 0.5 V. These preliminary studies had suggested that the reaction of $Li_2C_2$ described above would indeed occur in a Li-Al/iron sulfide cell and that $Li_2C_2$ would not re-form unless a very low cutoff potential (equal to or less than the emf of $Li_2C_2$) was used during subsequent discharges. The studies leading to the use of $Li_2C_2$ in Cell R-10 are described below.

The electrochemistry of lithium carbide* was investigated in Cell KA-1, which had a positive electrode consisting of 4.2 g of lithium carbide (nominally, 5.9 A-hr of lithium) in a graphite matrix, a negative electrode of Li-Al alloy and an electrolyte of LiCl-KCl. Cell KA-1 initially had an open-circuit potential of ∿1.0 V, which gradually decreased to ∿0.78 V upon standing for 1 hr. To evaluate the open-circuit potential of the cell further, the first charge cycle was interrupted and the cell was allowed to stand on open circuit for 10 hr. After this time, the open-circuit potential of the cell, that is, the emf of the $Li_2C_2$ *vs.* Li-Al was 0.78 V; this corresponds to an emf *vs.* Li of ∿1.08 V. The charge cycle was then completed using an IR-free cutoff potential of 1.89 V. The capacity measured during the cycle was approximately 5.7 A-hr. If the lithium carbide had been absolutely pure and had completely decomposed, 5.9 A-hr would have been required

*The lithium carbide used in these studies was prepared by Ventron Corp. and was the same material that had been used earlier (ANL-75-1, p. 117).

during the first charge cycle. Attempts to cycle the lithium carbide were only partially successful. During the two cycling studies, in which IR-free cutoff potentials of 1.88 and 0.20 V were used, the cell had a capacity of 1.8 A-hr with an ampere-hour efficiency of about 85%. Cell operation was terminated with the cell in the charged condition, and the lithium carbide electrode was replaced by a liquid lithium electrode. When the Li-Al electrode was discharged, 4.8 A-hr of lithium was transferred; this amount represents and increase of about 3.9 A-hr over the initial loading of lithium in the Li-Al electrode.

These results indicate that (1) a lithium carbide electrode operated *vs.* an electrode of Li-Al appears to be at least partially reversible, (2) the potential of the lithium carbide electrode *vs.* Li appears to be about 1.08 V, and (3) lithium carbide can be used as a source of additional lithium for uncharged Li-Al/iron sulfide cells.

2. Lifetime Studies
( W. R. Frost)

The objectives of these studies are to determine the cycle life of Li-Al alloy electrodes and to identify those factors that limit their cycle life. Investigations are being carried out in Li-Al/LiCl-KCl/Al cells to determine the effects of electrolyte purity, discharge current density, and cutoff voltage on the cycle life.

Cell LT-1 (ANL-75-36, p. 34) contained high-purity LiCl-KCl electrolyte from Anderson Physics Laboratory and was operated to provide base-line data on electrolyte purity. Cell LT-2 (ANL-76-9, p. 31) contained LiCl-KCl from Lithcoa; this electrolyte is of interest because of its lower cost. Both cells contained 26 A-hr of lithium as Li-Al alloy, and both were operated at a current density of 0.078 A/cm$^2$. Initially, both cells showed similar performance but after 30 cycles, the capacity of Cell LT-2 began a steady decline. At the end of 100 cycles, the lithium utilization of Cell LT-2 was about 15% lower than that of Cell LT-1. This decline in capacity has been attributed to the use of the lower purity electrolyte from Lithcoa.

Cell LT-2 has now operated for 4000 hr and 265 cycles, but the capacity continues to decline (the average utilization is about 53%). A reduction in ampere-hour efficiency after 100 cycles was corrected by reducing the cutoff potentials from 0.90 V to 0.35 V and operating the cell on open circuit between cycles. The cell will be operated for a total of 300 cycles and will then undergo a complete post-test examination.

3. Alternative Lithium Alloys for Negative Electrodes
(D. R. Vissers, W. R. Frost, K. E. Anderson)

Studies of lithium alloys other than lithium-aluminum are being conducted with the aim of identifying alloys that might serve as improved negative electrodes in lithium/iron sulfide cells.

Earlier studies (ANL-75-1, p. 47 and ANL-75-36, p.35) of lithium alloys including binary lithium-boron and lithium-silicon alloys and ternary alloys of lithium with silicon, boron, and aluminum indicated that lithium-

silicon alloy showed the greatest promise. Consequently, emphasis has been concentrated on the lithium-silicon system.

a. Lithium-Silicon Alloys

Earlier coulometric studies (ANL-75-36, p. 37) of the emf plateau regions of the Li-Si electrode identified the four lithium-silicon compounds formed (see Table IV-1). Recently, the plateau emfs were measured at four different temperatures (375, 400, 425 and 475°C) to determine the thermodynamic properties of the compounds; these are summarized in Table IV-2.

Table IV-1. Emfs of Active Materials in Li-Si Electrode and Proposed Chemical Compositions

| Plateau Emf, V, at 400°C (673 K) | Li-Si Atomic Ratios | | | Proposed Compound |
|---|---|---|---|---|
| | Cell I | Cell II | Average | |
| 0.049 | 3.63 | 3.82 | 3.73 | $Li_{15}Si_4$ |
| 0.161 | 2.92 | 2.97 | 2.94 | $Li_3Si$ |
| 0.281 | 2.02 | 2.03 | 2.03 | $Li_2Si$ |
| 0.336 | 1.45 | 1.42 | 1.43 | $Li_3Si_2$ |

Table IV-2. Thermodynamic Properties of the Proposed Lithium-Silicon Compounds at 400°C (673 K)

| Proposed Compound | -dE/dT, mV/K | $-\Delta G_f^\circ$, kcal/mol | $-\Delta H_f^\circ$, kcal/mol | $-\Delta S_f^\circ$, cal/(mol)(K) |
|---|---|---|---|---|
| $Li_{15}Si_4$ | 0.0949 | 77.70 | 108.76 | 46.15 |
| $Li_3Si$ | 0.1636 | 18.57 | 25.23 | 9.90 |
| $Li_2Si$ | 0.0611 | 14.86 | 18.99 | 6.13 |
| $Li_3Si_2$ | 0.1568 | 23.24 | 30.54 | 10.84 |

b. Ternary Lithium-Silicon-Metal Alloys

Performance characterization studies indicate that Li-Si alloy electrodes possess a high resistance and become seriously polarized during electrochemical transfer of lithium into and out of the electrode. Attempts are being made to identify and develop a ternary lithium-silicon-metal alloy that will improve the performance of the negative electrode. The systems presently being investigated include Li-$TiSi_2$, Li-$CoSi_3$ and Li-$VSi_2$. Preliminary results indicate these alloys are not superior to the binary Li-Si

alloy. Future studies will be carried out on other ternary lithium-silicon-metal alloy systems. This work will include continuing studies with the Li-Al-Si system, which was investigated earlier (ANL-75-36, p. 39).

4. Advanced Cell Designs
(D. R. Vissers, W. R. Frost, K. E. Anderson)

Work has recently been started on the development of a "button" cell which may be stacked in a bipolar array. The effort is concentrated on the development of ring seals and insulators, which are crucial to the successful development of such cells. Bipolar cell stacks have several potential advantages including (1) low fabrication costs, (2) high specific energy, and (3) elimination of the need for a feedthrough. The work is at a very preliminary stage and will be reported at a later date.

## REFERENCE

1. H. Shimotake and L. G. Bartholme, "Development of Uncharged Li-Al/FeS Cells," *Proc. Symp. and Workshop on Advanced Battery Research and Design*, p. B-210, ANL-76-8 (1976).

# V. ALTERNATIVE SECONDARY CELL SYSTEMS

(M. F. Roche, H. Shimotake, R. K. Steunenberg, W. J. Walsh)

The objective of this work is to develop new, secondary cell systems, with an emphasis on the use of inexpensive, abundant materials and either molten-salt or solid electrolytes. Cells employing calcium- or magnesium-based negative electrodes and molten-salt electrolytes are currently under investigation. Further studies may be extended to cells having other negative electrodes such as sodium or iron.

## A. Magnesium-Electrode Cells

(Z. Tomczuk, A. E. Martin, M. F. Roche)

A small $Mg/FeS_2$ cell with a 30 mol % NaCl-20 mol % KCl-50 mol % $MgCl_2$ electrolyte (mp, 396°C) was operated for nine discharge-charge cycles to test the rechargeability of this electrochemical couple. The negative electrode (4.5 A-hr capacity) was contained in a stainless steel housing with a 325-mesh stainless steel screen cover, and the positive electrode (1.0 A-hr capacity) was contained in a graphite cup with a graphite cloth cover. The exposed area of each electrode was 5 $cm^2$ and the current density was 10 $mA/cm^2$. Figure V-I shows a typical voltage-*vs.*-capacity curve for discharge and charge. The voltage plateaus at 1.53 and 1.10 V are in reasonable agreement with voltages calculated from free energy data[1] for the reactions $Mg + FeS_2 \rightarrow FeS + MgS$ (1.53 V) and $Mg + FeS \rightarrow Fe + MgS$ (1.16 V). The coulombic efficiency of the cell was over 90% initially, but after the fourth cycle it declined to 70% because of a short circuit. Magnesium dendrites, the probable cause of the

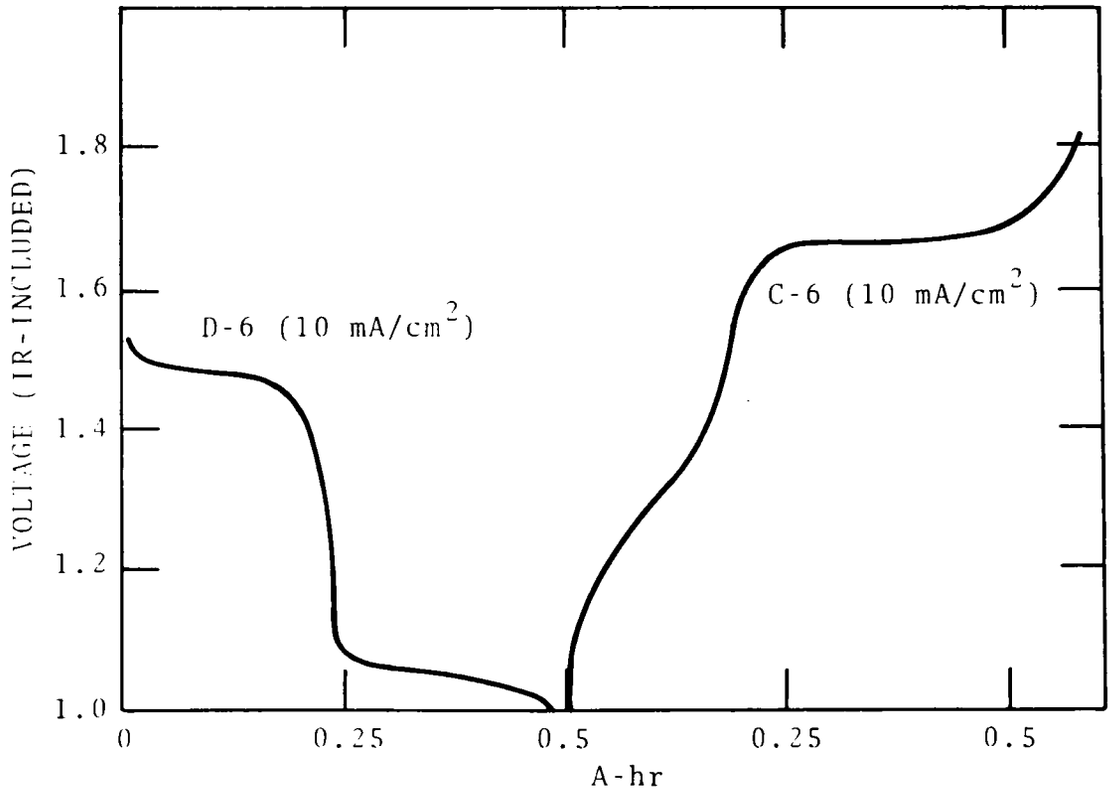


Fig. V-1. Discharge and Charge of a $Mg/FeS_2$ Cell (theoretical capacity, 1 A-hr; temperature, 450°C)

short circuit, were found on the stainless steel screen cover of the negative electrode. Means of avoiding the dendrite formation are under investigation.

B. Calcium-Electrode Cells
(M. F. Roche, S. J. Preto, L. E. Ross, A. E. Martin)

A small $Ca_2Si/Fe_3O_4$ cell was operated at 460°C for 22 charge-discharge cycles in an electrolyte (mp, 346°C) consisting of 8.7 mol % $CaCl_2$ in LiCl-KCl eutectic. The cell was started in the uncharged state (7.7 A-hr $CaSi_2$ in the negative electrode and 13.4 A-hr Fe + CaO in the positive electrode) and was cycled at current densities of 12.5 and 25 mA/cm$^2$. The electrodes were contained in 20-cm$^2$-area iron housings having zirconia-fabric and iron-screen covers for particle retention, and BN fabric was employed as a separator material. Cell voltage-*vs.*-capacity curves are shown in Fig. V-2. The cell had a cumulative A-hr efficiency of 90% and a total integrated discharge capacity of 68 A-hr. The capacity at 12.5 mA/cm$^2$ declined from about 5 to 3 A-hr over 20 cycles, and gas formation (which caused an increased resistance) was observed. The cell was evacuated occasionally to remove the gas and return the resistance to its normal value. It is suspected that gas formation, coulombic inefficiency, and capacity decline were all caused by the use of a high charge cutoff voltage (1.95 V); future cells of this type will employ more conservative charge conditions.

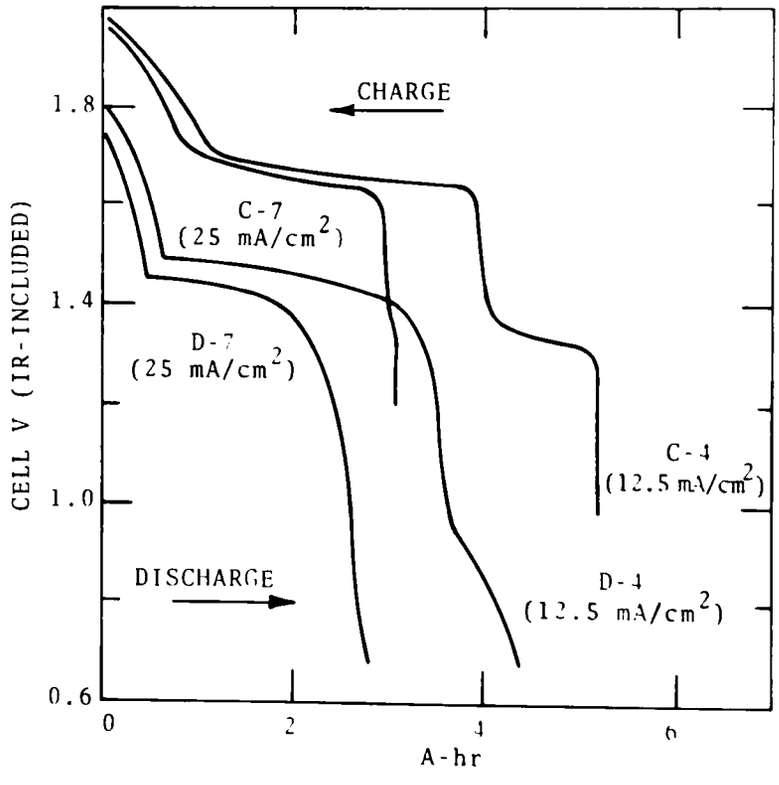


Fig. V-2. Discharge and Charge of a $Ca_2Si/Fe_3O_4$ Cell (theoretical capacity, 7.7 A-hr; temperature 460°C; resistance, 120 mΩ)

The cycling behavior of calcium/iron sulfide laboratory-scale cells is summarized in Table V-1. The cells with $CaCl_2$-NaCl electrolyte have two problems, both of which are associated with the negative electrodes. In the Ca-Al electrode, charging to the preferred calcium-rich compound, $CaAl_2$, has not yet been demonstrated. (The compound, $CaAl_4$, which has been identified in the electrode by metallographic and X-ray techniques, has too high an equivalent weight for a practical cell.) Three $Ca_2Si$ cells were operated, and all had poor coulombic efficiencies (about 85%). The poor coulombic efficiencies of these cells, which are operated in stainless steel beakers, have been attributed to the sodium vapor produced when the compound $Ca_2Si$ is in contact with $CaCl_2$-NaCl electrolyte. A thermodynamic calculation of the sodium vapor pressure over this mixture gave a value of 1.4 Torr. (The calculation is based on the 150-mV difference in potential between the compound and a sodium-pool electrode in $CaCl_2$-NaCl electrolyte at 550°C.) More detailed studies of the Ca-Al and Ca-Si electrodes are being undertaken to determine whether the two problems discussed above can be circumvented.

The cells listed in Table V-1 that employed a $CaCl_2$-LiCl-KCl electrolyte (5 mol % $CaCl_2$ in LiCl-KCl eutectic) operated reasonably well at current densities up to 160 mA/cm$^2$. However, operation of these laboratory-scale cells has suggested some areas of possible improvement. For example, electrolyte mixtures higher in $CaCl_2$ concentration are now being tested to determine whether cell polarization can be improved; in these cells, polarization is about twice that observed in comparable Li-Al/FeS cells.

Table V-1. Cycling Data for Ca-Al/FeS and Ca-Si/FeS Cells

| Composition and Capacity[a] | Cycles | A-hr Eff., % | Total A-hr Discharged |
|---|---|---|---|
| **$CaCl_2$-NaCl Electrolyte (550°C)** | | | |
| $CaAl_4$ (3)/FeS (11) | 14 | 98 | 38 |
| $Ca_2Si$ (11)/FeS (9) | 8[b] | 85 | 32 |
| **$CaCl_2$-LiCl-KCl Electrolyte (460°C)** | | | |
| $CaAl_2$ (15)/FeS (15) | 36 | 99+ | 253 |
| $Ca_2Si$ (20)/FeS (15) | 15 | 99+ | 130 |
| $Ca_2Si$ (20)/FeS (15)[c] | 33 | 96 | 270 |

[a]Numbers in parentheses indicated the capacity (in A-hr) of each electrode.

[b]This cell was terminated because of marked decline in capacity (others terminated for metallographic examination).

[c]Assembled in uncharged state.

Metallographic and X-ray* analyses showed that the major compounds in the negative electrode were $CaAl_2$, $CaAl_4$ and CaSi, and in the positive electrodes, FeS, Fe and CaS. The calcium-rich compound $Ca_2Si$ (1.65 V *vs.* FeS) was difficult to recharge completely in these cells. Reasonable charge-cutoff voltages (1.85 V, IR-included, at 20 $mA/cm^2$) typically produced CaSi (1.35 V *vs.* FeS) as the major compound in the charged negative electrode. Electrolytes richer in $CaCl_2$, which are now being tested, may improve the rechargeability of $Ca_2Si$.

C. Prismatic Cell Tests
(H. Shimotake, W. A. Kremsner)

Two Ca/iron sulfide prismatic cells of intermediate scale were fabricated and operated at 450°C. Both were uncharged cells with LiCl-KCl-5 mol % $CaCl_2$ electrolyte. Cell CA-1 (7.5 by 12.5 by 2.5 cm) had a single positive electrode of 28 A-hr capacity that contained a mixture of CaS and iron and copper powders. (The weight ratio of iron to copper was 7 to 3.) This positive electrode was placed between two $CaSi_2$ negative electrodes. The total $CaSi_2$ capacity was 25 A-hr, assuming that the $CaSi_2$ is charged to CaSi. A lack of compactness in the design led to a low specific energy (34 W-hr/kg at the 12-hr rate), but the cell performance was very stable. Utilization varied from 57% at 10 $mA/cm^2$ to 40% at 50 $mA/cm^2$ (current densities are based on an active area of 120 $cm^2$). Operation of this cell was continued for 55 cycles and 1000 hr, with no decline in capacity before voluntary termination. However, metallographic examination indicated settling of active material and a reaction in the negative electrode between the active material and the Retimet current collector.

Cell CA-2 (7 by 10 by 4 cm), which was also assembled uncharged, had five electrodes (3 negatives and 2 positives) and an interelectrode area of 240 $cm^2$. The total capacity of the negative electrodes was 60 A-hr and that of the positive electrodes, 69 A-hr. The positive electrodes initially had the same composition as that of Cell CA-1, and the negative electrodes were pressed aluminum plaques. This cell is still undergoing testing. Problems with electrode matching, aggravated by a minor short circuit between one of the positive electrodes and the facing negative electrodes, have limited the cell performance to 36 W-hr/kg at the 12-hr rate. Various modifications in cell design are being tested in an effort to improve the cell performance; these will include the use of an electrolyte with a higher $CaCl_2$ concentration and tests of other negative-electrode compounds.

*X-ray analyses performed by B. S. Tani, Analytical Chemistry Laboratory, ANL.

## REFERENCE

1. J. F. Elliott and M. Gleiser, *Thermochemistry for Steelmaking*, Vol. 1, pp. 245-247, Addison-Wesley Publishing Co., Inc., London (1960).